J Neurophysiol 95: 284–300, 2006.
First published September 14, 2005; doi:10.1152/jn.01329.2005.

Temporal Evolution of 2-Dimensional Direction Signals Used to Guide Eye Movements

Richard T. Born,[1] Christopher C. Pack,[3] Carlos R. Ponce,[1] and Si Yi[2]

[1]*Department of Neurobiology, Harvard Medical School, Boston, Massachusetts;* [2]*Harvard University, Program in Mind, Brain and Behavior, Cambridge, Massachusetts; and* [3]*Montreal Neurological Institute, McGill University, Neurology and Neurosurgery, Montreal, Quebec, Canada*

Submitted 22 December 2004; accepted in final form 6 September 2005

Born, Richard T., Christopher C. Pack, Carlos R. Ponce, and Si Yi. Temporal evolution of 2-dimensional direction signals used to guide eye movements. *J Neurophysiol* 95: 284–300, 2006. First published September 14, 2005; doi:10.1152/jn.01329.2005. The smooth pursuit system must integrate many local motion measurements into a coherent estimate of target velocity. Several laboratories have studied this integration process using eye movements elicited by targets, such as tilted bars, containing conflicts between local motion signals measured along *contours* [one dimensional (1D)] and those measured at the bar's endpoints, or *terminators* [two dimensional (2D)]. The general finding is that 1D signals dominate early responses, whereas later components of the behavior are determined by 2D signals. We studied the dynamics of the integration process in macaque monkeys by systematically varying the relative proportions of 1D and 2D signals and the retinal eccentricities at which they appeared. Predictably, longer bars produced greater and longer-lasting contour-induced deviations. The evolution of the 2D response occurred over a period of 50–400 ms, depending on the relative proportions of 1D and 2D signals. As contours were displaced from the fovea the deviation decreased but much less so for early (1st 40 ms) than for late (subsequent 40 ms) pursuit initiation. These bottom-up effects could be overcome to a limited extent by the top-down influence of predictability. Finally, we observed that when animals were free to track any part of the bar, they spontaneously made short-latency saccades to the terminators on most trials, especially when the bars were tilted. This suggests an increased saliency of moving terminators, particularly when discrepancies exist among local motion signals.

INTRODUCTION

Everything that the primate brain can know about the visual world is represented on ~2 million more-or-less discrete channels—the fibers of the optic nerves. Each one of these channels contains a limited amount of information about a very small part of the visual field, defined as the receptive field of a single retinal ganglion cell. While the fine grain of this representation is essential for high acuity vision, the limited nature of the subunits poses a problem for the rest of the visual system. How are the parts of the image that belong together integrated into coherent representations of objects?

One way of thinking about the spatially limited receptive fields of retinal ganglion cells is as "apertures," which create local visual signals that are frequently ambiguous. This is easy to imagine for any moving object that has edges at oblique angles with respect to its direction of motion (Fig. 1*A*). A neuron with a small receptive field positioned along the contour of one of these edges can measure only the component of motion perpendicular to the contour. Such a one-dimensional (1D) measurement is inherently ambiguous because it is consistent with many possible directions of actual object motion. In contrast, neurons whose receptive fields are positioned over two-dimensional (2D) features, such as the object's corners or endpoints ("terminators") can measure the direction of object motion accurately. Thus the visual motion system is often presented with a conflict[1] between the potentially erroneous 1D signals measured along a contour and the veridical 2D signals originating from terminators. How is this conflict resolved?

Microelectrode recordings from neurons in the middle temporal visual area (MT) of alert monkeys have shown that the earliest directional responses, beginning ~80 ms after the onset of stimulus motion, are strongly biased by 1D motion but that the later responses encode the 2D direction of motion, regardless of contour orientation. Thus the responses of MT neurons reflect the gradual evolution of a solution to the aperture problem for motion over a period of ~60–100 ms (Pack and Born 2001). The time course of the neural solution can be longer or shorter, depending on the length of the bars and their contrast (Pack and Born, unpublished observations), and it is also strongly affected by general anesthetics (Born et al. 2002; Pack et al. 2001).

Given the evidence that MT neuronal signals are important for the initiation of smooth pursuit and other smooth eye movements (Born et al. 2000; Groh et al. 1997; Komatsu and Wurtz 1989; Newsome et al. 1985), it is not surprising that a similar effect has been observed behaviorally (Masson and Castet 2002; Masson and Stone 2002; Masson et al. 2000; Pack and Born 2001). Thus smooth pursuit provided us with a tool for examining the temporal properties of motion integration as we varied different stimulus parameters, such as bar length, eccentricity, and the predictability of the direction of target

[1] From a strictly geometric perspective, there is no "conflict" because the local motion signals are created by a single, rigidly translating object. However, when one considers the signals from direction-selective neurons with small receptive fields, there is a conflict because the neurons with receptive fields restricted to the contour will signal a different direction of motion—namely the one perpendicular to the contour—than would neurons with receptive fields positioned over the terminators. That there is in fact a directional conflict in the brain is evidenced by the initial misperception of such motion (Lorençeau et al. 1993) and by the eye movement phenomena that are the subject of this report.

Address for reprint requests and other correspondence: R. T. Born, Dept. of Neurobiology, Harvard Medical School, Boston, MA (E-mail: rborn@hms.harvard.edu).

The costs of publication of this article were defrayed in part by the payment of page charges. The article must therefore be hereby marked "*advertisement*" in accordance with 18 U.S.C. Section 1734 solely to indicate this fact.

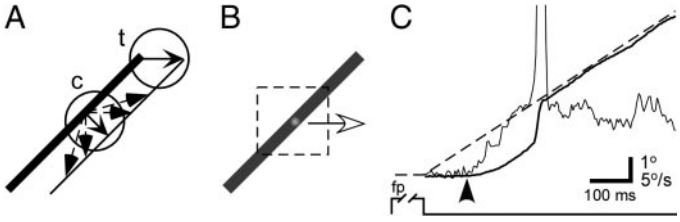

FIG. 1. General methods. *A*: aperture problem for visual motion. The thick and thin oblique lines represent 2 successive snapshots of the bar moving to the right. The circles represent the receptive fields of neurons early in the visual pathways, such as those in V1. Due to the limited size of these receptive fields, the motion signals measured along the contour (c) are ambiguous because the observed displacement is consistent with an infinite number of possible displacements over a range of 180°. Motion signals measured at terminators (t) do not suffer from this problem. *B*: visual stimulus consisted of a green bar on which was superimposed an isoluminant red Gaussian blob. The subject was required to track the center of the bar to within 2–3°, indicated by the dashed square. This "target window" was not visible to the subject, and it moved with the target. *C*: pursuit data from a single trial from one monkey showing both the horizontal eye position (thick line) and velocity (thin line) superimposed on the trajectory of the target position (dashed line). The onset of pursuit (arrow head) is most clearly seen in the velocity trace.

motion. Some portions of this work have been described briefly in previous publications (Born and Pack 2002; Born et al. 2002; Pack and Born 2001).

METHODS

Surgical preparation

Seven adult rhesus monkeys (*Macaca mulatta,* 6 male, 1 female) were surgically prepared for chronic behavioral experiments and then trained to perform a fixation task and a visual tracking task. Four of these monkeys were used for the various bar *pursuit* experiments (Table 1). The other three were used for the experiments in which we examined the nature of *saccades* made to moving bars (Figs. 10–14). The experimental protocols were approved by the Harvard Medical Area Standing Committee on Animals. In a sterile surgical procedure under isoflurane anesthesia, a coil of fine wire was implanted between the conjunctiva and the sclera for the measurement of eye position (Judge et al. 1980; Robinson 1963). During the same surgical procedure, stainless steel or titanium bone screws were implanted in the skull and a fixture for immobilizing the head was attached using dental acrylic.

Behavioral paradigm

The animals were placed on a controlled fluid intake schedule and received water or juice as reinforcement during training and experimental sessions. Monkeys were first trained to pursue a small red spot. The animals foveated the fixation point (a small red square, 11 arc-min on a side, luminance 20.6 cd · m^{-2}) for a randomly varied period of 500-1,300 ms at the end of which the fixation point disappeared, and, simultaneously, a red spot (0.5° diam) appeared at the fixation location and began to move in one of several possible directions and speeds. After the animals were proficient at tracking the red spot, the target was changed to a long green bar with the same red spot superimposed on its center (Fig. 1*B*). Initially the bar was made quite dim and the spot very bright, but even so, the natural tendency of the monkeys was to saccade to one of the bar's terminators and track this feature (see following text). To discourage this tendency, we limited the computer-controlled eye-position window to a small area (±2 or 3° for longer bars) centered on the spot. If the monkey failed to track the spot or made a saccade to one of the terminators, which were always located well outside of the target window, the visual stimulus was extinguished, no reward was given, and a brief time-out was inserted before the start of the next trial.

In a typical experiment, such as the one for which results are shown in Figs. 2 and 3, the bar could move in one of four different directions (right, left, up, or down) at 10° · s^{-1} and at one of three possible relative orientations (perpendicular, or tilted +45 or −45° with respect to the direction of motion) for a total of 12 different motion conditions. For each possible trial type, we generally performed 20–30 repetitions in a blockwise random order.

Visual stimuli

Visual stimuli were presented on a Mitsubishi monitor (70 × 52 cm, 57 cm away; 1 pixel subtended ~0.1°) at a refresh rate of 60 Hz. The bar was dim green (4.2 cd · m^{-2}; $u' = 0.28$, $v' = 0.59$), its center was indicated by an isoluminant, red Gaussian blob (4.2 cd · m^{-2}; $u' = 0.64$, $v' = 0.34$; sigma = 0.2°), and it moved against a black background (0.06 cd · m^{-2}). Values for chrominance and luminance were measured with a PR-650 SpectraScan Colorimeter (Photo Research; Chatsworth, CA) (CIE 1932). The subject had to track the center of the bar to within ±2° (Fig. 1*B*) while eye movements were monitored using a scleral search coil. The bars used for the "naïve" experiments (Figs. 10–14) were the same color green but lacked the red spot. For the experiments involving a "precue" as to the direction of motion, the cue consisted of a bright white arrow (90 cd · m^{-2}; $u' = 0.19$, $v' = 0.45$) that appeared for ~300 ms at the beginning of the fixation period. The tail of the arrow originated at the fixation point and its head pointed in the direction of target motion on the upcoming trial. Cued and un-cued trials were randomly interleaved.

Data analysis

Eye position and velocity (analog differentiator: low-pass, –3 dB at 50 Hz) were digitized and stored to disk at 250 Hz for off-line analysis (Fig. 1*C*). Saccades were automatically detected using a previously published algorithm (Krauzlis and Miles 1996), and individual trials were rejected from further analysis if a saccade occurred within the first 80 ms of pursuit. For smooth pursuit, later-occurring saccades were removed and filled in with "NaNs," which were then treated as missing values in subsequent analyses. The time of pursuit onset was detected using a modification (Madelain and Krauzlis 2003) of the algorithm published by Carl and Gellman (1987). Pursuit onset was determined as the intersection of two regression lines, one fit to the baseline and one fit to the response eye velocity data. The baseline was defined as the time from 40 ms prior to the onset of target motion to 40 ms after; the response was taken as the 40 ms of data from the point at which the eye velocity exceeded the baseline by 3 SDs. From this point of intersection, we then explored 40 ms in either direction to determine whether another hinge point provided a better fit to the data, in a least-squares sense. Each trial was then displayed with markers for saccades and the onset of pursuit so that it could be visually inspected and the markers adjusted by the operator if necessary.

TABLE 1. *Monkeys participating in different experiments*

Monkey	Bar Length	Eccentricity	Bar Width	Direction Cue	Blocked	Naïve
H	X	X	X	X	X	
B		X	X	X	X	
C	X	X	X			
G	X	X				
F						X
I						X
J						X

For quantitative analysis of early (or late) pursuit, we used the first (or 2nd) 40 ms of eye velocity after the onset of pursuit. The data from each trial were fit with a least-squares regression line, and the slope of this line was used as the measure of eye acceleration during that period. The individual slope values (i.e., accelerations) were then used for further statistical analyses. For many experiments, this consisted of a multi-way ANOVA using the "anovan" function in Matlab (The Mathworks, Natick, MA) with a constrained (Type III) sums of squares. Post hoc comparisons were made with the "multcompare" Matlab function using the "Tukey-Kramer" correction for critical values. Comparisons across subjects were performed using a one- or two-factor repeated measures ANOVA (RMANOVA) (Trujillo-Ortiz et al. 2004a,b).

For the analyses of the angular deviation of pursuit, the direction of the eye velocity vector was determined for each successive pair of time points (Δt = 4 ms) on each trial. The directional components of the velocity vectors across many trials were then analyzed using methods of circular statistics (Zar 1996) to determine the mean angle and the corresponding 95% confidence intervals. Significance testing of angular data were performed using the Watson-Williams two-sample test for circular data. We also fit each curve of angular deviation over time (e.g., Fig. 3*C*) with exponential decay functions of the general form

$$D = A_o*[\exp(-t/\tau_1) + \exp(-t/\tau_2). . . + \exp(-t/\tau_n) + C$$

where D is the observed angular deviation over time, t, and the free parameters are the initial amplitude, A_0, a constant offset, C, and the various time constants, $\tau_{1\text{-}n}$. Fits were optimized with a least squares criterion using the Levenberg-Marquardt algorithm (Matlab's "lsqcurvefit"). Each data set was first fit with a single and double exponential, and the errors of the two fits were compared using a sequential F-test (Draper and Smith 1966). If the addition of the second exponential significantly improved the fit ($P < 0.05$), a third exponential was added, the sequential F-test repeated, and so on. In practice, no more than two exponential terms were ever justified. Once the optimal model was determined in this way, 95% confidence intervals for each parameter were determined using a bootstrap procedure (Efron and Tibshirani 1993) in which the raw data were re-sampled, a new angular deviation curve was generated and re-fit. By repeating this procedure 1,000 times, we generated a distribution of bootstrap parameters from which SEs and confidence intervals were derived.

For the "naïve" bar-pursuit experiments (Figs. 10–14), latency distributions were compared using the Wilcoxon rank-sum test ("ranksum" function in Matlab), and probabilities of making saccades to terminators were compared directly using the binomial distribution. In general, we determined the probability, P, of observing x or more saccades on n trials for tilted bars, if the underlying probability, p, of making such a saccade was that determined from the nontilted bar trials. Using the Matlab statistics toolbox, this corresponds to: $P = 1 - \text{binocdf}(x - 1, n, p)$. Two-dimensional saccade histograms (Figs. 10, 11, and 14) were generated by counting the number of saccades made to each location (spatial bins: 0.05 × 0.05°) and smoothing with a 2D Gaussian of sigma = 0.35°. The location of each saccade was plotted relative to the location of the bar at the time of the saccade, and the coordinates were rotated so that saccades to leading terminators were upwards and those to trailing terminators were downwards. For maps in which data were pooled for bars of different lengths (Fig. 11), saccade distances were scaled by bar length prior to binning and smoothing.

RESULTS

All monkeys reliably pursued the tilted bar targets and revealed a contour-induced deviation in pursuit initiation as predicted by the aperture problem. Figure 2 shows an example of this effect for one monkey (*H*) for one direction of bar motion (rightward at 10°/s). In this case, for either tilt condition, the *horizontal* component of the contour direction is identical (rightward, Fig. 2*A*), but the *vertical* component is in opposite directions: upward for a tilt of +45° (Fig. 2*B,* red traces) and downward for a tilt of −45° (Fig. 2*B,* blue traces). Thus the contour-induced deviation is manifest in the axis of pursuit perpendicular to the axis of bar motion, and can be seen reliably even in the raw eye position traces (Fig. 2*B*). The timing of the deviation is seen more clearly in the eye velocity traces (Fig. 2, *C* and *D*), whose vertical components begin to diverge ~125 ms after the onset of target motion. When the orientation of the bar was perpendicular to its direction of motion (nontilted control, Fig. 2, *C* and *D,* green traces), there was no conflict between local and global motion signals and the animals' pursuit was veridical. That is, the initial direction of pursuit was purely in the direction of bar motion, and there was no component of pursuit perpendicular to this direction.

For each trial, we determined the *perpendicular* eye acceleration (see METHODS) over the first 40 ms of pursuit and used this as a measure of the effect of local, contour-related motion

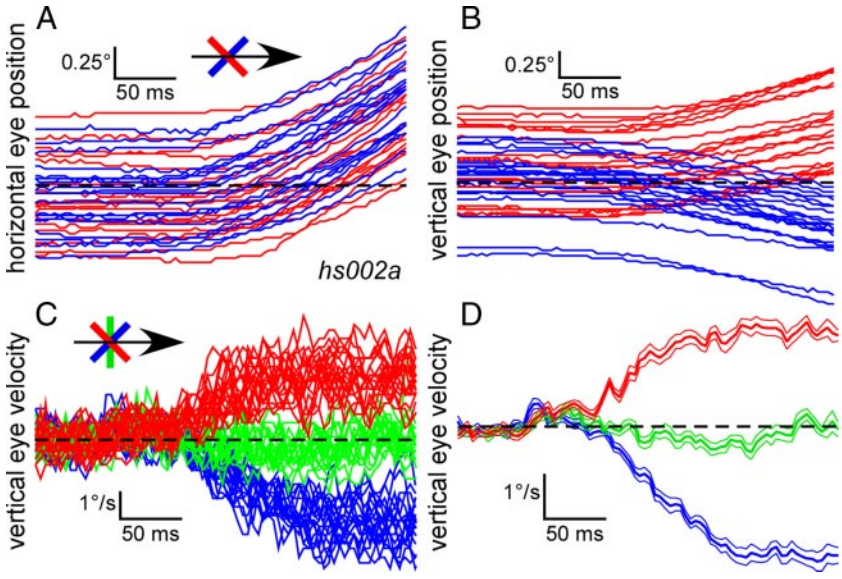

FIG. 2. Bar pursuit data from *monkey H* for 1 direction of target motion. *A* and *B*: individual horizontal (*A*) and vertical (*B*) eye position traces for trials in which the target moved to the right at 10° · s^{-1} but was tilted either +45° (red, n = 20 trials) or −45° (blue, n = 19). The control trials (vertical bar) are omitted here for clarity but are shown in *C* and *D. C*: vertical eye velocity shown for the same trials as in *B* but with the addition of the control (green, n = 17) trials in which the bar's orientation was perpendicular to its direction of motion. *D*: averages (thick lines) of the data shown in *C;* thin lines indicate the SE.

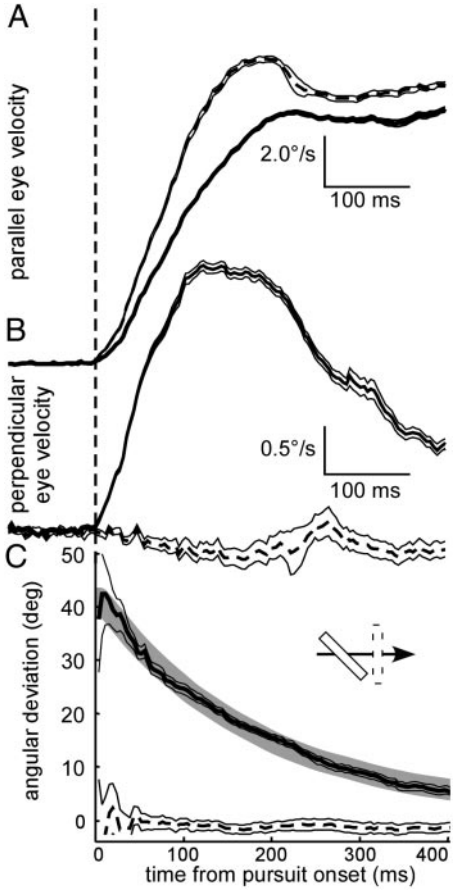

FIG. 3. Pooled bar pursuit data from 1 experiment for *monkey H*. Eye velocity parallel (*A*) or perpendicular (*B*) to the direction of target motion for tilted (solid lines; $n = 908$ trials) vs. perpendicular (dashed lines; $n = 437$ trials) bars. The vertical dashed line indicates the time of pursuit onset. *C*: summary plot of the average angular deviation (thick lines) and the corresponding 95% confidence intervals (thin lines) for tilted bars (solid) and nontilted controls (dashed). The thick gray line is the best-fitting single-exponential decay function (see METHODS). Numbers of trials for each condition are the same as in *A* and *B*.

signals. For the experiment shown in Figs. 2 and 3, we randomly interleaved four different directions of bar motion (right, left, up, or down) at one of three possible relative tilt angles (no tilt or a tilt of +45° or −45°) for a total of 12 different conditions. After aligning the eye velocity data on the initiation of pursuit, we analyzed the deviation across all conditions using a two-way ANOVA. For this experiment, there was a highly significant effect of bar tilt ($P < 0.0001$) and a nonsignificant effect of direction of motion ($P > 0.1$) as well as a nonsignificant interaction between the two factors ($P > 0.1$). The mean pursuit deviations for the different bar tilts are summarized in Table 2. The pursuit deviations induced by the +45 and −45° bar tilts were, on average, nearly identical in magnitude but opposite in sign (Fig. 2*D*), so that the absolute values of the effects were not significantly different (*t*-test, $P > 0.3$).

Because similar effects on pursuit deviation were seen regardless of the absolute direction of bar motion (right, left, up, or down) or the *sign* of the bar tilt (+45 or −45° with respect to the direction of bar motion), we combined data across all eight of these conditions to show the net deviation in pursuit performance over many trials (Fig. 3). This was accomplished by using the components of eye velocity perpendicular and parallel to the *direction of bar motion* and inverting the sign of the perpendicular component for the −45° condition. Figure 3 shows that the initial pursuit of a tilted bar deviates from the true direction of motion, thus producing a substantial component in the direction perpendicular to that of the target motion. The deviation in the direction perpendicular to the true direction of motion (Fig. 3*B*) is accompanied by a commensurate slowing of the pursuit in the same direction as that of bar motion (Fig. 3*A*) as one would expect from the geometry of the tilted bars. Indeed, the two traces (tilted bar and control) in Fig. 3*A* superimpose if the control traces are multiplied by the cosine of 45° (0.707). This latter fact was not indicated in a preliminary report of this finding (Pack and Born 2001), but it is clearly a feature of the data. The component of pursuit *parallel* to the direction of target motion did not differ for the +45 and −45° conditions (*t*-test, $P > 0.4$).

The actual *direction* of the initial deviation in pursuit velocity is rendered explicitly in Fig. 3*C*. To combine the direction of pursuit deviation across trials having different absolute directions of bar motion, we again calculated the direction of the eye movement *relative* to the direction of motion of the bar. In these plots, zero deviation always corresponds to veridical pursuit (i.e., in the direction of bar motion). As we would expect, the pursuit of the nontilted control bars shows no angular deviation (dashed line of Fig. 3*C*). For each time bin, we calculated the mean directional deviation across trials and the 95% confidence interval (thin lines in Fig. 3*C*) based on the von Mises distribution (Zar 1996; p. 604–605). Prior to the onset of pursuit (<100 ms after the onset of target motion), the measured directions of eye movement are essentially random, thus producing extremely large confidence intervals, and are not shown. This picture of the data indicates that the earliest pursuit deviates *nearly* 45°, that is, perpendicular to the orientation of the bar, presumably as a consequence of the aperture problem. Comparing this vector plot with the more traditional Cartesian representation in Fig. 3, *A* and *B*, reveals an important feature of the data, which is that the angular deviation decreases over time initially because the component of eye speed parallel to the bar's direction of motion is increasing more rapidly than is the perpendicular component—note the difference in velocity scales for the two components. Even 150 ms after pursuit onset there is an appreciable perpendicular component (Fig. 3*B*), which, for the long bar (34°) used in this experiment did not disappear completely for another 350 ms. The time course of the angular deviation was well described ($r^2 = 0.994$) by a single exponential with a time constant of 180 ms (Fig. 3*C*, gray line). Finally the same initial deviation in pursuit was seen under less-constrained conditions during experiments in which the green bar contained no red spot and

TABLE 2. *Perpendicular eye accelerations for monkey H during early (1st 40 ms) and late (2nd 40 ms) of pursuit initiation*

	Early Pursuit	Late Pursuit	No. of Trials
No Tilt	0.00 ± 0.88	0.00 ± 0.95	437
+45°	+24.27 ± 0.86	+20.58 ± 0.97	451
−45°	−23.89 ± 0.87	−18.52 ± 0.96	457

Values are means ± SE in °/s^2.

the animals were free to make saccades to any part of the bar (as described in the following text; Fig. 10*E*).

Effect of bar length

The data presented in the preceding text, as well as that previously published for perception (Lorençeau et al. 1993), smooth pursuit in monkeys (Pack and Born 2001) and humans (Masson and Stone 2002), and ocular following in humans (Masson and Castet 2002; Masson et al. 2000), are consistent with the idea that early responses reflect the contributions of *both* contour- and terminator-related motion signals. If this idea is correct, one straightforward prediction is that the behavior should be affected by the relative proportion of contour and terminator present in the stimulus. A simple way to test this is to vary the *length* of the bar used as a pursuit target. Any single bar has only two terminators, but increasing the length adds progressively more contour-related signal. As a result increasing the bar length should increase the magnitude of the initial pursuit deviation or prolong its time course or both.

To test this prediction, we repeated the previous experiment with bars of different lengths presented on randomly interleaved trials. Increasing bar length had the expected effect of increasing the contour-based deviation according to several different measures of the behavior (Fig. 4). We performed this experiment in each of three monkeys (*C, G,* and *H*), and all showed a similar increased deviation with increased bar-length. A two-way RMANOVA (bar length and tilt) on the perpendicular pursuit acceleration revealed a nonsignificant main effect of bar-length ($P > 0.5$), a highly significant effect of tilt ($P < 0.001$), and, most critically, a highly significant interaction between bar length and tilt ($P < 0.00001$).

As noted in the preceding text, the magnitudes of the deviations between the +45 and −45° conditions were not significantly different (*t*-test, $P > 0.1$), so we averaged them together for presentation of the results. Figure 4*A* shows the *relative pursuit deviation* for each different bar length in one monkey (*H*). The overall magnitude of the initial deviation in eye velocity was clearly greater for longer bars (Fig. 4*A*) as was the initial eye acceleration (measured as the slope of the 1st 40 ms of pursuit), and this trend was consistent for all three monkeys (Fig. 4*B*). The component of pursuit *parallel* to the direction of bar motion was not significantly affected by the length of the bar (2-way RMANOVA, $P > 0.1$). Vector plots of the de-saccaded data aligned on pursuit onset revealed that the *direction* of pursuit was similarly affected by bar length. For *monkey H,* the effect ranged from a maximum of near 45°

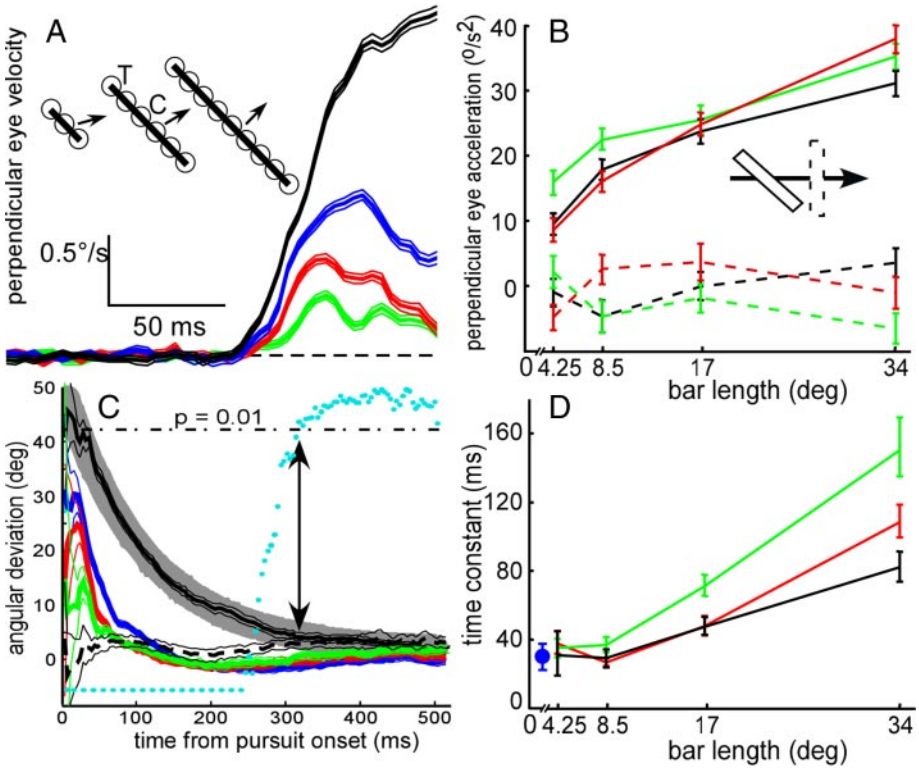

FIG. 4. Results of varying bar length. *A*: average eye velocity perpendicular to the direction of target motion for bars of different lengths for *monkey H.* Each thick line is the average of ~900 trials; thin lines represent SE. *B*: initial (from 0 to 40 ms after pursuit onset) perpendicular eye acceleration as a function of bar length for 3 different monkeys (*C,* green; *H,* red; *G,* black) for bars that were either tilted (solid lines) or not (dashed lines). The error bars indicate SE. *C*: time course of the angular deviation for bars of different lengths in *monkey H* (same data as in *A*). The thick lines represent the direction of the mean vector and the thin lines represent the 95% confidence interval about the mean direction. The cyan circles plot the *P* values of a 2-sample test (Watson-Williams test) at successive time points comparing the deviation induced by the longest tilted bar (solid black line) with the nontilted bar of the same length (dashed black line). The time at which the difference becomes nonsignificant (arrows) was defined as the duration of the deviation. The significance criterion, $P = 0.01$, is represented by the horizontal dash-dot line. Symbols near the bottom of the plot correspond to a $P < 10^{-14}$. *D*: time constants of the best-fitting single-exponential decay as a function of bar length for the same 3 monkeys (colors as in *B*). Error bars indicate 95% confidence intervals determined using a bootstrap procedure (see METHODS). The filled blue circle indicates the best-fitting time constant for the population data for 60 MT cells recorded from 2 alert macaque monkeys. The fit was to the angular deviation of the mean neuronal direction vector in response to fields of tilted bars, each bar being 3° long (Fig. 2C from Pack and Born 2001).

with the longest bar to a minimum of ~13° for short bars (Fig. 4*C*). The other monkeys followed the same pattern, with *monkey C* showing slightly larger effects at all bar lengths. The *duration* of the directional deviation was also affected by bar length (Fig. 4*C*). We obtained an objective measure of the duration by finding the time point at which the angular deviation for tilted bars was no longer significantly different from the corresponding nontilted bar condition ($P > 0.01$, Watson-Williams test).[2] This type of comparison is illustrated in Fig. 4*C* for the longest bar. The difference between the deviation induced by the 34°-long tilted bar (solid black line) is significantly different from the control (dashed black line) beginning at the onset of pursuit and remains significant for ~300 ms thereafter. The filled circles of Fig. 4*C* represent the *P* values of the Watson-Williams test as a function of time, and the point at which they cross the significance criterion of 0.01 (horizontal dash-dot line) was defined as the duration of the tilt effect. For this measure, all three monkeys exhibited the same monotonic increase in contour-effect duration as bar length was increased.

This effect on the duration of the angular deviation was also clear in the exponential functions fit to the curves of angular deviation versus time (Fig. 4*C*). The majority of these curves (37/48) were adequately described by a single exponential (sequential *F*-test, $P > 0.05$). For experiments in which the addition of a second exponential significantly improved the fit, the difference between the two fits was extremely subtle and bore no systematic relationship with bar length (χ^2 test for homogeneity, $P > 0.3$). We thus used the best-fitting first-order exponential for comparisons across conditions and found, as for the other measures, that the time constants generally increased with bar length (Fig. 4*D*). This was not true, however, for the two shortest bar lengths (4.25 and 8.5°) for which the distributions of time constants were not significantly different (paired *t*-test, $P > 0.3$). For comparison, we have also plotted the time constant of an exponential fit to the population data for 60 MT cells recorded from two alert macaque monkeys (Fig. 2C of Pack and Born 2001).

Effect of eccentricity

If the contour-induced deviation in pursuit is caused by the spatially delimited receptive fields of visual neurons, then one might predict that increased stimulus eccentricity would diminish the tilt effect. The rationale for this prediction is illustrated in Fig. 5*A*, which shows why the larger receptive field sizes at greater eccentricities, e.g., (Daniel and Whitteridge 1961; Gattass and Gross 1981) might have the effect of tipping the balance in favor of the terminator-based motion signals. Put another way, presenting a bar of constant length at a greater eccentricity effectively shrinks the visual representation of the stimulus, making it more like a spot or a blob (Lorençeau et al. 1993), which might also be expected to reduce deviation due to the aperture effect.

[2] This use of a two-sample hypothesis test is obviously not strictly correct as we do not adjust for multiple comparisons nor do the successive time bins represent independent samples. We use this metric more as a descriptive statistic—an objective way to determine when the two curves no longer differed. In every case, the differences were obvious from visual inspection and sustained across multiple time bins. Measuring them "by eye" would not have produced any different conclusions.

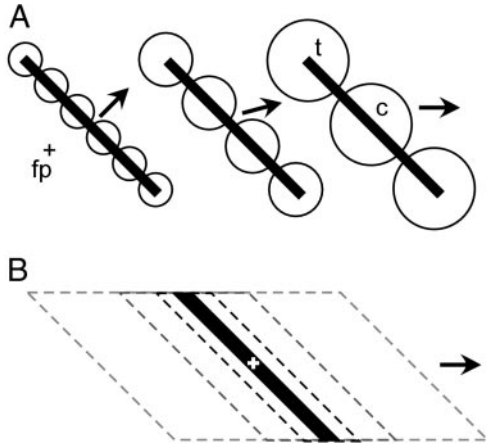

FIG. 5. *A*: logic of the eccentricity experiments. As a bar of constant length is presented at greater distances from the fovea, the apertures (receptive field sizes, indicated by circles) grow larger and give progressively greater weight to terminators (t) relative to contours (c), according to the relative numbers of "units" of each type activated. This might be expected to progressively diminish the contour induced deviation, as indicated by the direction of the arrows. *B*: visual stimuli (not drawn to scale) used for the bar width experiments shown in Fig. 8. Each stimulus was a parallelogram centered on the fixation point, was of the same uniform (green) color, and had the same fuzzy, red spot at its center. In this type of stimulus, the edges defining the contour are symmetrically displaced from the fovea, and the top and bottom edges (except at the corners) give no motion information since they are parallel to the direction of motion (indicated by the arrow).

To test this prediction, we conducted two different experiments. In the first, using four monkeys (*B, C, H,* and *G*), we presented bars of different lengths, as in the preceding text, but also varied the eccentricity at which the bar appeared. To make the results at different eccentricities directly comparable, we wanted to use stimuli moving at the same speed ($10° \cdot s^{-1}$) and to examine pursuit that occurred prior to any saccades that would place the target on the fovea. These exigencies limited the range of eccentricities that we could test and further required us to analyze only trials in which the target moved back toward the fovea so that there was a significant period of presaccadic pursuit (Rashbass 1961). Nevertheless, this experiment allowed us to compare directly the same stimuli presented at different eccentricities on randomly interleaved trials.

Results for two eccentricities and three different bar lengths are shown for one monkey in Fig. 6. It is immediately apparent that the effect of bar length described in the preceding text (Fig. 4) is reproduced at both eccentricities as the deviated component (Fig. 6, *A* and *B, bottom*) increases with increasing bar length. In addition, a comparison of the two families of curves suggests that eccentricity had the expected effect—the curves produced by bars presented 4° off of the fovea (Fig. 6*B*) clearly have decreased slopes compared with their counterparts at 2° of eccentricity (Fig. 6*A*). However, as is apparent in Fig. 6, *A* and *B, top,* the component of eye velocity *parallel* to the direction of target motion also decreased with eccentricity. This had the net effect of rendering the angular deviation roughly equivalent across different eccentricities, at least for the early period of open-loop pursuit.

There were subtle differences in the time course of the behavior, however, as revealed by exponential fits to the angular deviation for individual experiments. For these experiments in which we compared two eccentricities for multiple bar lengths, there were fewer trials for each condition (between

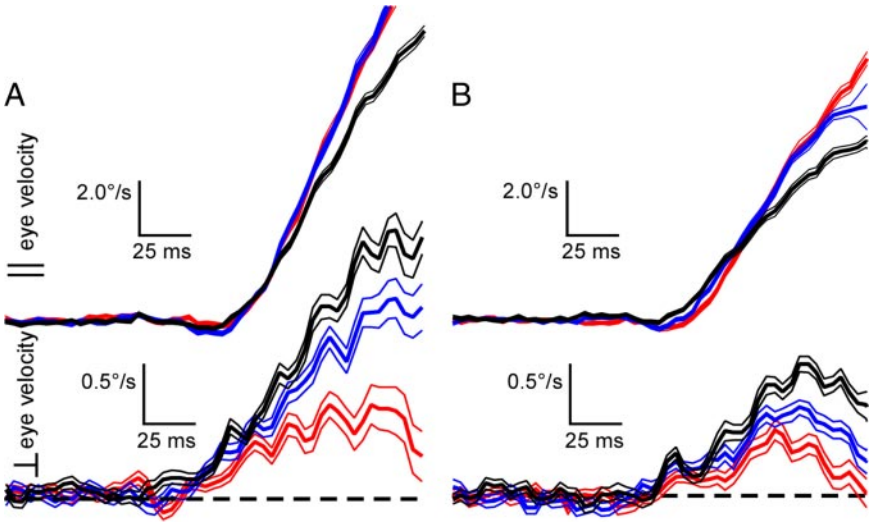

FIG. 6. Effects of eccentricity on the contour-induced deviation of smooth pursuit initiation. *A* and *B*: direct comparison of parallel (*top*) and perpendicular (*bottom*) eye velocities presented at 2 different eccentricities (2°, *A,* and 4°, *B*) for 3 different bar lengths (8.5°, red; 17°, blue; 34°, black) in *monkey H.* Each thick trace represents the average of ~80 trials; thin lines are ±SE.

60 and 70), hence the angular deviation curves were noisier. As a result, we obtained satisfactory exponential fits ($r^2 > 0.9$) for *both* eccentricities for only 31 of 71 (44%) of the experiments. Of these 31 experiments, for nearly every comparison (29/31) the time constant for the target at the *greater* eccentricity was *smaller* than that for the same stimulus appearing at a lesser eccentricity (Fig. 7*A*; sign test, $P < 0.0001$). Even when we relaxed our criterion for goodness of fit ($r^2 > 0.8$) or eliminated it completely so that all comparisons were included, the same trend remained highly statistically significant ($P < 0.0001$). This trend became more obvious when we pooled data for the same eccentricity and monkey across different experiments. By

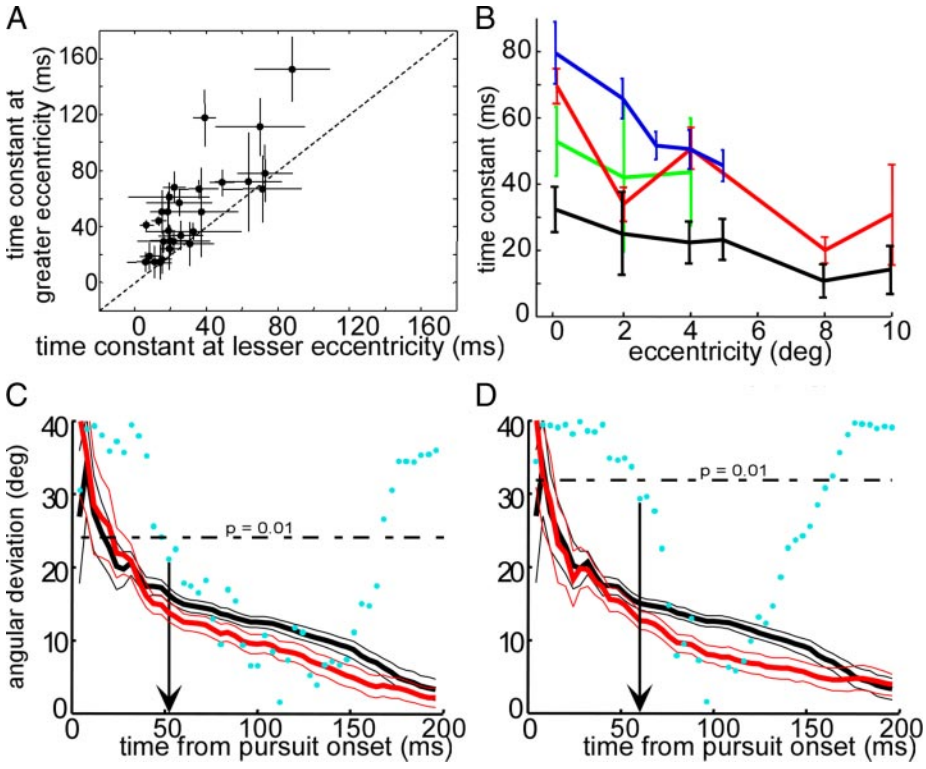

FIG. 7. Effects of eccentricity on the angular deviation of pursuit initiation. *A*: for experiments in which 2 different eccentricities were randomly interleaved, single-exponential decay functions were fit to the angular deviation curve for each eccentricity. Each filled circle ($n = 31$) indicates the time constant of the fit to the angular deviation curve for the lesser (abscissa) vs. the greater (ordinate) eccentricity. Eccentricity differences ranged from 2 to 6°. Error bars show SE for each fit, determined using a bootstrap procedure. *B*: time constants of the exponential decay function fit to the pooled data for each monkey (*monkey B,* blue; *C,* green; *H,* red; *G,* black) at each eccentricity tested. Error bars represent SE. *C* and *D*: angular deviation as a function of time for the pooled data from *monkey H* comparing the deviation for foveally presented 34°-long bars vs. the same bars presented at 2° (*C*) or 4° (*D*) from the fovea. The 0° eccentricity data are based on 470 trials, and the 2° and 4° data are based on 232 and 352 trials, respectively. Eye-movement data were first de-saccaded and then aligned on pursuit onset. The magnitude of the deviation was significantly reduced for eccentrically presented bars, but the two curves do not diverge significantly until >50 ms after pursuit onset (arrows). Thick lines represent the direction of the mean vector; thin lines show the 95% confidence interval. The filled cyan circles plot the significance values for the Watson-Williams test comparing the 2 angular distributions at each time point. The horizontal dash-dot line represents the significance level of $P = 0.01$; symbols near the bottom of the plot correspond to a P value of 10^{-5} (*C*) or 10^{-10} (*D*).

so doing, we were able to obtain robust measures of the time constant and 95% confidence intervals as a function of target eccentricity. All four animals had a negative slope to the regression line fit using maximum likelihood, and the regression was statistically significant for three of the four animals ($P < 0.01$; for *monkey C,* $P = 0.60$; Fig. 7*B*). Thus we conclude that, for these experiments, increasing the eccentricity did reduce the magnitude of the angular deviation, albeit in a rather subtle way.

To analyze in finer detail the temporal aspects of the eccentricity effect, we directly compared the angular deviations at different eccentricities as a function of time (Fig. 7, *C* and *D*). We calculated the time from pursuit onset to the point at which the two angular deviation curves became significantly different (arrows in Fig. 7, *C* and *D*) from the same 71 experiments in four monkeys. In 35 cases, no statistically significant differences were obtained between the two curves. In the remaining 36 cases, the differences were always in the predicted direction—that is, the angular deviation was decreased at the nonzero eccentricity—however, the differences did not emerge until the later phase of pursuit initiation. The earliest divergence we observed occurred 44 ms after pursuit onset, and the average was considerably longer than this [mean = 98 ± 10 (SE) ms; median = 72 ms]. This *late* effect of eccentricity stands in marked contrast to that of bar length, where the differences were apparent as soon as pursuit began (Fig. 4).

The preceding results suggested that eccentricity had very little effect on the early period of pursuit initiation, but that it did alter later phases of the response. However, the geometric limitations of the experiment made it difficult to reach a firm conclusion for later periods of pursuit—due to the intrusion of saccades—and for greater eccentricities. We therefore conducted a second series of experiments using bars of a single length (34°) but of varying *widths*, which had the effect of symmetrically displacing the edges of the bars various distances from the fovea (Fig. 5*B*). The "bars" for these experiments were actually parallelograms—the end contour was parallel to direction of bar motion—so that we did not add potentially disambiguating contour signals along the ends. As before the parallelograms were a uniform green color, but contained an isoluminant red gaussian blob at its center. These experiments were performed with three of the four pursuit monkeys (*C, H,* and *B*).

Increasing the bar's width had the effect of diminishing contour-induced deviations at greater eccentricities, while leaving the component parallel to the direction of bar motion relatively constant (Fig. 8*A, top*; RMANOVA, $P > 0.1$). This produced more reliable differences in the pursuit behavior over longer time periods because the animals made very few saccades. As in the previous experiment, the earliest phase of pursuit showed only a very small effect of eccentricity, with larger differences emerging after the first 40 ms of pursuit. This can be seen in the averaged perpendicular eye velocity traces (Fig. 8*A*), which nearly superimpose over the first 40–50 ms of pursuit and only diverge after this point (arrow). A two-way RMANOVA (tilt and bar width) revealed the expected significant main effect for tilt and a highly significant interaction term ($P < 0.00001$) for both early (1st 40 ms) and late (2nd 40 ms) pursuit. That the effect of bar width on early pursuit was small is shown more clearly by plotting the perpendicular eye acceleration as a function of contour eccentricity for the early versus late phases of pursuit initiation. For early pursuit initiation, this function is nearly flat, whereas for the later period the effect is considerably greater (Fig. 8*B*). The difference in slopes was highly significant (*t*-test, $P < 0.001$) both for the pooled data shown in Fig. 8 as well as for each individual experiment in all three monkeys ($P < 0.05$; 4 each in *monkeys B* and *H;* 6 in *monkey C*). The same trend was seen in the vector plots, with subtle—but significant—effects of eccentricity in all three animals (Fig. 8, *C* and *D*; linear regression, $P < 0.05$). Thus this second experiment confirms the main result of the first, which is that eccentricity does diminish the

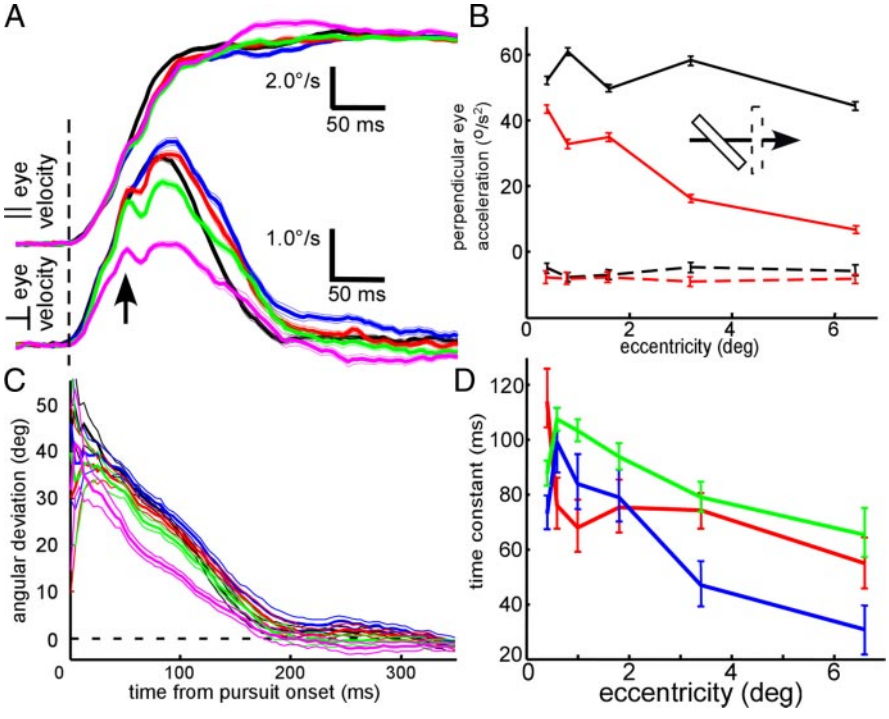

FIG. 8. Results of bar width experiments. *A*: magnitude of the eye velocity parallel (*top*) or perpendicular (*bottom*) to the direction of target motion for parallelograms of different widths corresponding to different contour eccentricities : 0.4°, black; 0.8°, blue; 1.6°, red; 3.2°, green; 6.4°, magenta. For example, the stimulus for the condition listed at an eccentricity of 6.4° was a parallelogram that was 12.8° wide and centered on the fovea at the time of motion onset. The long side of each parallelogram measured 34°. Each thick line is the mean of ~970 trials, and thin lines represent the standard error of the mean. *B*: effect of eccentricity on the *early* (black, 1st 40 ms of pursuit) and *late* (red, 2nd 40 ms of pursuit) phases of pursuit initiation. In each subplot, the slope of the eye velocity data shown in *A* is plotted against the eccentricity of the parallelogram's contours for both tilted (solid lines) and nontilted (dashed lines) targets. Error bars represent SE. *C*: mean angular deviation of pursuit over time for the same stimuli. Conventions are as for *A*. Thick lines show the direction of the mean vector during each 4-ms bin; thin lines represent the 95% confidence interval of the mean direction. *D*: time constants of the exponential decay function fit to the pooled data for each monkey (*monkey B,* blue; *C,* green; *H,* red) at each eccentricity tested. Error bars represent SE.

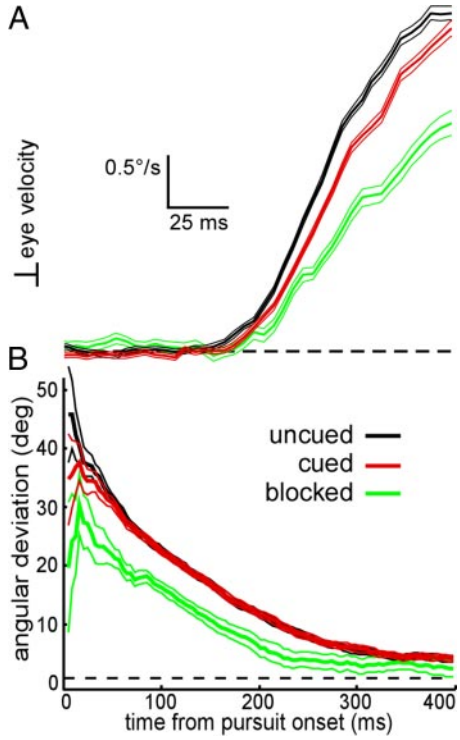

FIG. 9. Effect of directional predictability on the contour effect. For all plots, black lines indicate trials in which the direction of motion was unpredictable, red lines indicate trials in which a direction cue preceded the appearance of the target, and green lines indicate trials that were performed in blocks containing the same direction of motion on every trial. *A*: perpendicular eye velocity for the different cue conditions from 1 monkey (*H*); mean ± SE. (uncued, 1,020 trials; cued, 1,014 trials; blocked, 316 trials). *B*: angular deviation for the same data in *A*. Thick lines indicate the direction of the mean vector and thin lines represent the 95% confidence interval about the mean direction.

contour effect for tilted bar pursuit, but predominantly for the latter half of pursuit initiation.

Effect of predictability

The preceding experiments indicate that ambiguous local motion signals emanating from contours are manifest in the initiation of smooth pursuit eye movements and that these ambiguities exist because of the limited size of receptive fields at early stages of the visual pathways. Thus the contour effect for pursuit can be thought of as a signature of "bottom-up" motion processing. It is also clear, however, that both pursuit behavior (e.g., Deno et al. 1995) and motion perception (e.g., von Grunau et al. 1998) are subject to more cognitive, "top-down" influences, such as those following from the predictability of target motion. Given this duality of influences on the behavior, we thought it would be interesting to pit them against each other to ask to what extent prior knowledge of target direction could reduce the ambiguities inherent in early visual motion processing.

We did this by giving the monkeys information regarding the true direction of target motion well before it began to move. Insofar as this information can influence pursuit, it should diminish the deviation caused by the orientation of the tilted bars. For this experiment, bar motion on any given trial could be in one of four possible directions and at one of three possible relative orientations as described in METHODS. The new feature was that on a randomly chosen half of the trials, target onset was preceded by a cue—an arrow pointing away from the fixation spot—that indicated the upcoming direction of target motion. The cue appeared during the first 300 ms of the fixation period, and was then extinguished prior to an additional 500–1,300 ms of fixation before target onset. Thus although the direction of target motion was predictable on these trials, the time of its appearance was not. This experiment was performed in each of two monkeys (5 experiments in *monkey B* and four in *monkey H*).

The cue had a statistically significant effect for both monkeys but only for the early phase (1st 40 ms) of pursuit initiation (Fig. 9, *A* and *B*; 2-way RMANOVA, $P < 0.001$). Importantly, in every case the effect of the cue was to *decrease* the perpendicular component (Fig. 9*A*, Table 3), while leaving the *parallel* component of pursuit unchanged (cue-tilt interaction $P > 0.3$ for both early and late pursuit initiation). The cue effect was quite subtle, however, producing only a very small and short-lived (from 0 to 12 ms after pursuit onset) decrease in the angular deviation (Fig. 9*B*).

The small size of the effect of target predictability for monkeys was difficult to interpret, however, because we had no independent evidence that the monkeys understood the cue's meaning. Even though they were rehearsed for many trials during which the cue was consistently paired with the direction of target motion, it was still easy for them to do the task correctly without paying any attention to the cue. Moreover, there was no external incentive for them to improve their pursuit by minimizing the deviation.

To address this issue, we performed an additional experiment in which target motion predictability was created by repeating the same direction of target motion in *blocks* of trials. In these experiments, we continued to vary the relative orientation of the bar, but the speed and direction were constant within a block of 200–300 trials. In separate blocks of trials, we collected data from different directions of target motion so that the overall data set was matched to that for the cued versus un-cued experiments. This manipulation had the effect of greatly reducing the contour-induced deviation as shown by the green traces in Fig. 9, *A* and *B*. Both the initial perpendicular eye acceleration (Fig. 9*A*) and the angular deviation (Fig. 9*B*) were considerably smaller. For angular deviation, this difference, with respect to both the cued and the un-cued data, was highly significant ($P < 0.01$, Watson-Williams test) for all time points out to 300 ms after pursuit onset. Exponential fits to the angular deviation curves revealed a similar story: the time-constants for both monkeys were nonsignificantly reduced by the presence of the cue, and there was a large and statistically

TABLE 3. *Perpendicular eye accelerations for cued and non-cued trials*

	Monkey H		*Monkey B*	
	−Cue	+Cue	−Cue	+Cue
No tilt	0.00 ± 0.80	0.00 ± 0.80	0.00 ± 1.43	0.00 ± 1.45
+45°	24.97 ± 0.79	23.31 ± 0.80	33.95 ± 1.38	32.73 ± 1.38
−45°	−27.91 ± 0.79	−24.49 ± 0.79	−43.22 ± 1.38	−37.08 ± 1.39

Values are means ± SE in °/s^2.

significant effect of the block design (τ_{nocue} = 124 ± 9 ms; τ_{cue} = 116 ± 7 ms; $\tau_{blocked}$ = 100 ± 6 ms).

Saccades to tilted bars: the salience of terminators

For all of the experiments presented thus far, we required the animals to track the approximate center of the bars and enforced this by using an eye-position window centered on the spot. We did this because it was obvious in our first training attempts that, regardless of the salience of the spot, the monkeys tended to make saccades to the endpoints of the bar. This tendency seemed potentially interesting because it suggested a particular visual salience of terminator-related motion signals. We therefore studied it in three additional animals (*monkeys F, I,* and *J*), who were naïve to the bar-pursuit task. All three animals were well trained on the pursuit of small spots but had never before pursued bars. For these experiments, we made the eye-position window large enough so that eye movements made to any point along the bar were permitted. We used bars of moderate length (9.4° for *monkey F;* 9.4 and 18.8° for *monkeys I;* and 8.5 and 17° for *monkey J*) and, as in previous experiments, randomly interleaved four different directions of target motion and three different relative bar orientations.

Representative eye traces from *monkey F* for the subset of trials on which the bars moved upwards at $10° \cdot s^{-1}$ are shown in Fig. 10*A*. The traces show the horizontal eye position over time for cases in which the bar was tilted either +45° (blue) or −45° (red) with respect to the direction of bar motion, or not tilted (black). On almost every trial, the animal made an early saccade to one of the bar's endpoints. For this particular direction of motion, the saccade was made to a *leading* terminator on nearly every trial—that is, when the bar was tilted +45° (blue lines), the saccade was made to the right-hand terminator, which was displaced from the bar's center in the *same* direction as the bar was moving. This was not always the case, however, as most monkeys had general directional biases for saccades. For example, *monkey F* showed a mild, but significant, bias for left- over rightward saccades (measured across all trial types, $P > 0.05$, binomial test) and an extremely strong tendency to make upward over downward saccades ($P < 0.0001$, binomial test). This meant that, for rightward bar motion, for example, he made saccades nearly exclusively to the trailing terminator for +45° tilts (73 of 74 trials) and to the leading terminator for −45° tilts (61 of 62 trials). In both cases, the terminator chosen was the one above the center of the bar regardless of whether it was leading or trailing with respect to the direction of bar motion. However, when the different directions of bar motion were balanced, all three monkeys did show a weak overall tendency to saccade to leading terminators: *monkey F,* 58% leading ($P < 0.0001$, binomial test); *monkey I,* 57% leading ($P < 0.0001$, binomial test); *monkey J,* 52% leading ($P = 0.13$, binomial test).

Another feature of the data in Fig. 10*A* is that the saccades appear to occur earlier and with greater frequency when the bar was tilted compared with when it was not. To examine this tendency across different directions of bar motion, we determined the percentage of trials on which the animal made a saccade to within 2° of one of the bars' endpoints within a time window from 100 to 400 ms after the onset of bar motion. The data for the 9.4° long bar are shown as a polar histogram in Fig. 10*B* in which different directions around the circle indicate the direction of bar motion, and the differently colored symbols indicate the relative orientation of the bar. The data indicate that the animal frequently made short-latency saccades to the bars' endpoints when the bar was tilted but was less likely to do so when the orientation of the bar was perpendicular to its direction of motion. To assess the significance of this differ-

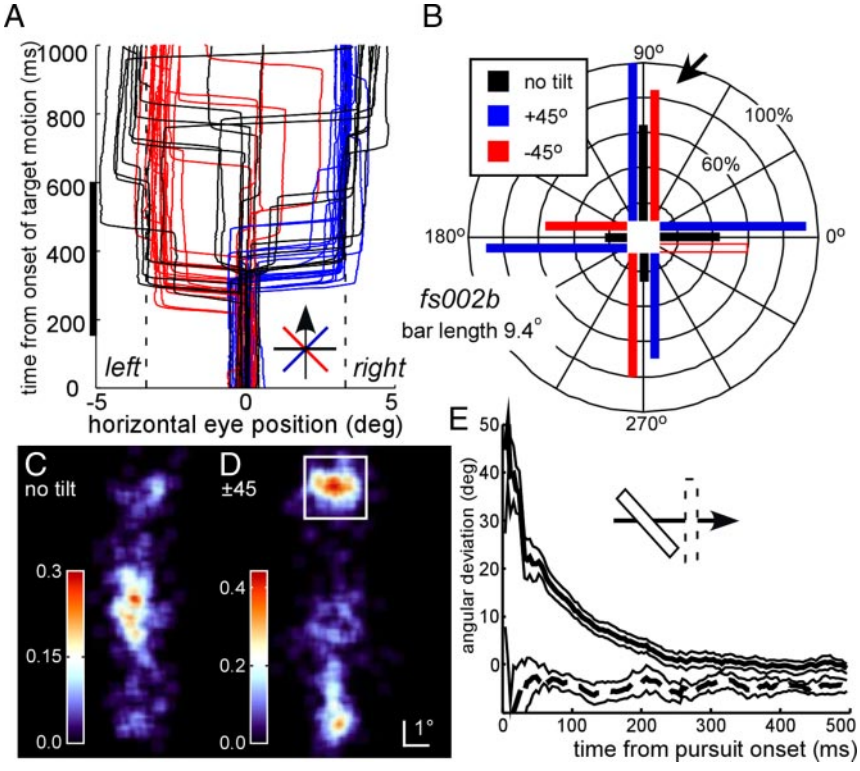

FIG. 10. Saccades during tracking of tilted bars by "naïve" animals. *A*: horizontal eye position traces from ~20 trials each of bars tilted either +45° (blue) or −45° (red) or nontilted (black). For these trials, the bars always moved straight upward. The rightward and leftward deflections represent saccades to one of the bar's terminators, which are shown by the dashed lines. *B*: polar histogram of the percentage of trials on which the animal made a saccade to within 2° of the bars' endpoints over an interval from 100 to 400 ms after the bar began to move. The direction of each set of three bars indicates the direction of target motion; the different colors represent different relative bar orientations. Solid red and blue bars indicate cases in which the number of saccades to a tilted bar was significantly greater ($P < 0.01$, binomial test) than would be expected by chance if the probability of a saccade was the same as that on control (nontilted bars) trials. *C* and *D*: 2-dimensional histograms of the saccade endpoints for all saccades made between 100 and 400 ms after motion onset of 9.4° bars that were either nontilted (*C,* 351 saccades) or tilted ±45° (*D,* 602 saccades). The color of each pixel indicates the number of saccades made to that location. The numbers along the color axis are small because the pixels (bins) are small. For a sense of scale, the box around the location of the leading terminator contains 246 saccades. *E*: angular deviation plots of smooth pursuit during the same trials, after de-saccading and aligning on the initiation of pursuit. Thick lines indicate the direction of the mean vector and thin lines represent the 95% confidence interval about the mean direction.

ence, we used the binomial distribution to determine the probability of obtaining a number of saccades equal to or greater than the number observed for the tilted bar condition if the underlying probability were that observed for the corresponding nontilted bar (see METHODS). For seven of the eight possible comparisons in Fig. 10*B*, this difference in saccade behavior evoked by perpendicular bars versus tilted bars was highly significant (binomial test, $P < 0.01$). Only for rightward moving bars tilted −45° was the number of saccades to terminators not significantly greater than for perpendicular bars ($P = 0.13$, indicated by the *unfilled* red bar in Fig. 10*B*).

The enhanced salience of the terminators of tilted bars is shown even more clearly in 2D maps of saccade frequency (Figs. 10, *C* and *D*, and 11). We generated these maps by plotting the location of *every* saccade made by the monkey as a function of the position of the center of the bar with all coordinates rotated so that, for tilted bars, saccades to leading terminators were upward and those to trailing terminators were downward. Figure 10, *C* and *D*, shows saccade maps for *monkey F* for a bar length of 9.4° for all saccades made between 100 and 400 ms after the onset of bar motion. For nontilted bars, most of the early saccades were made to regions near the center of the bar, whereas for tilted bars, the endpoints were more often targeted. This was true for all monkeys and both bar-lengths as shown in Fig. 11. For all of the tilted bars, the vast majority of saccades, whether early or late, were made to terminators (Fig. 11, *B* and *D*). For the nontilted bars, only at later times after motion onset were a significant proportion of saccades made to the terminators (Fig. 11*C*).

The differences in the *timing* of the animals' tendency to make saccades to terminators are shown in more detail in Fig. 12. For each trial, we detected each saccade and determined whether or not the eye landed within 2° of one of the bar's terminators. For trials containing saccades to terminators, we then measured the time of initiation of the first such saccade with respect to the beginning of target motion and defined this as the "saccade-to-terminator (STT) latency." Figure 12*A* shows histograms of these latencies for *monkey F* for bars 9.4° long. The blue and red distributions, reflecting STT latencies for bars tilted +45 and −45°, respectively, are clearly well to the left of the distribution for nontilted bars. This can be better appreciated in a normalized cumulative distribution plot (Fig. 12*B*), which shows the curve for nontilted bars (black line) well to the right of those for tilted bars. Both distributions, however, fail to indicate the trials on which the animal made *no* saccades to the terminators at any time. The proportion of trials with no STT are shown as *insets* in Fig. 12, *B–D*, and they indicate another major feature of the data, which is that monkeys are much less likely to saccade to a terminator when the bar is not tilted. Data from the other two monkeys are shown in Fig. 12, *C* and *D*, for two different bar lengths: *monkey I* (Fig. 12*C*) 9.4° (solid lines and bars) and 18.8° (dashed lines, hollow bars); *monkey J* (Fig. 12D) 8.5° (solid lines and bars) and 17.0° (dashed lines, hollow bars). In each case, note that the black curves lie to the right of their colored counterparts and the black bars indicating trials with no STTs are larger. Thus all three monkeys showed the same tendency to make *early* STTs far more frequently when the bars were tilted compared with when they were not ($P < 0.01$, Wilcoxon rank-sum test; median values in Table 4) and to make STTs on a far greater proportion of trials with tilted bars ($P < 0.01$, binomial test).

One potential difficulty in interpreting the difference in STTs for tilted versus nontilted bars stems from the fact that the bars were the same length for all conditions of tilt. This meant that, for tilted bars, the *perpendicular* distance from the bar's center to one of its terminators was shorter, by a factor of 0.707 (cosine of 45°). Thus although the absolute magnitude of any STT was the same regardless of tilt condition, the fact that

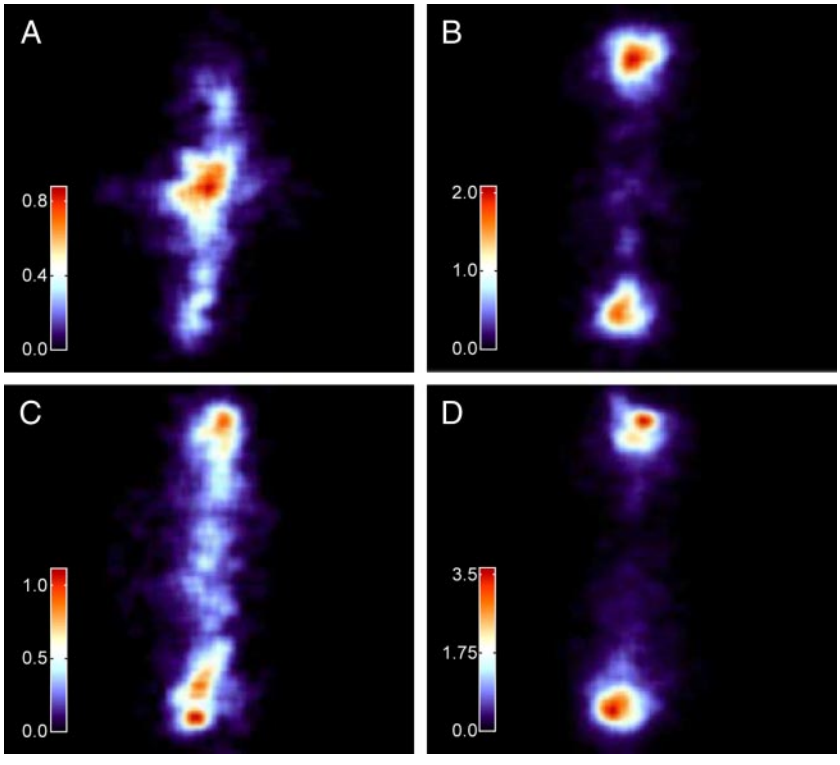

FIG. 11. Two-dimensional histograms for all saccades made by all 3 monkeys (*I, J,* and *K*). *A*: map of early saccades (between 100 and 400 ms after the bar began moving) to nontilted bars (1,543 saccades). *B*: map of early saccades to bars tilted ±45° with respect to their direction of motion (2,987 saccades). *C*: map of late saccades (between 400 and 1000 ms after the bar began moving) to nontilted bars (2,353 saccades). *D*: map of late saccades to tilted bars (4,233 saccades).

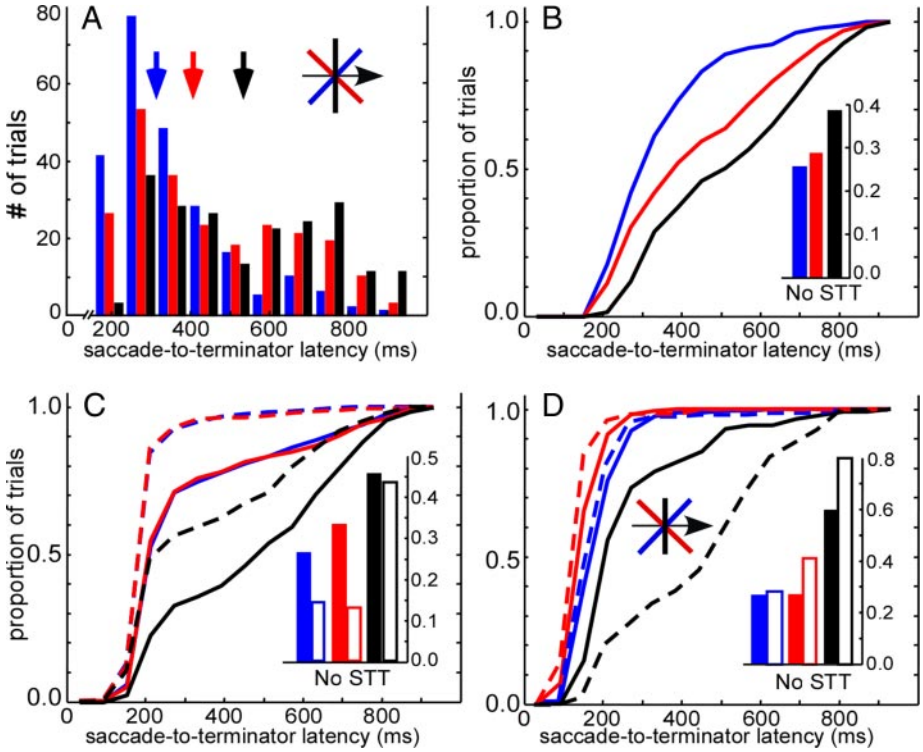

FIG. 12. Latency of saccades-to-terminators (STTs). The time of initiation of each saccade made to a point within 2° of one of the bar's endpoints was determined for each trial. For all plots, blue indicates trials on which the bar was tilted +45°; red, −45°; and black, nontilted. *A*: STT latency histogram for *monkey F*. The bars were 9.4° long for all trials, and each condition's histogram is based on 360 trials. *B*: cumulative density functions for the data shown in *A*. *C*: cumulative density functions of STT latency for *monkey I* for each of two different bar lengths: 9.4° (solid lines and filled bars) and 18.8° (dashed lines and hollow bars). *D*: cumulative density functions of STT latency for *monkey J* for each of 2 different bar lengths: 8.5° (solid lines and filled bars) and 17° (dashed lines and hollow bars). For *monkey J*, the control (nontilted) bars were shortened to 6° and 12°, respectively. The bar plots of each *inset* (*B–D*) indicate the proportion of trials on which no saccade was made to a terminator (no STT). Values for the median of each distribution and the number of trials on which it is based are given in Table 4.

the component perpendicular to the direction in which the animal was already pursuing was shorter for tilted bars may have made them more attractive targets on this basis alone. To examine this possibility, we shortened the nontilted bars so that the perpendicular distance was now the same for all conditions for one monkey (*J*). This manipulation had no effect on the behavior, as the same differences between tilted and nontilted bars were evident (Fig. 12*D*). The STT latency distributions from the *same* monkey with and with-out the shorter nontilted bars were indistinguishable ($P > 0.1$, Wilcoxon rank-sum test) as was the probability of making a STT ($P > 0.1$, binomial test).

The preceding results show that monkeys are more likely to saccade to a terminator when there is a *discrepancy* among local motion measurements (tilted bars) compared with when there is no discrepancy (nontilted bars). This could result either because such a discrepancy actively promotes saccades or because consistency actively suppresses them. In either case, the behavior would require a rapid estimate of the reliability of local motion signals. Alternatively, it is possible that there is something inherently more interesting about corners of *oblique* objects. Recall that our stimuli always moved in one of the four cardinal directions of motion. Thus nontilted bars were oriented either vertically or horizontally, whereas tilted bars always had an oblique orientation.

TABLE 4. *Median STT latencies (s) for the distributions shown in Fig. 12*

Monkey (Bar Length)	*F* (9.4°)		*I* (9.4°)		*I* (18.8°)		*J* (8.5°)		*J* (17.0°)	
	Median	*n*	Median	*n*	Median	*n*	Median	*n*	Median	*n*
No tilt	0.532	360	0.508	457	0.252	459	0.224	220	0.506	219
+45°	0.316	360	0.240	458	0.208	459	0.180	218	0.168	220
−45°	0.406	360	0.236	459	0.204	460	0.136	217	0.136	219

STT, saccade to terminator.

To distinguish between these possibilities, we performed two additional control experiments. In the first, we randomly interleaved trials on which the bar appeared centered on the fovea but remained stationary. On these trials, the bars' shapes and orientations were identical to the corresponding trials on which the bar moved, but there were no motion signals, hence no discrepancy. We reasoned that insofar as motion signals were the basis of the differences between STTs of tilted versus nontilted bars, the difference should disappear on the static trials. This prediction was borne out by the data (Fig. 13, Table 5). The distribution of STT latencies for nontilted bars largely overlapped with those of tilted bars on the static trials (Fig. 13; moving bar data are represented by dashed lines and hollow bars; stationary bar data are represented by solid lines and solid bars) and the difference in the probability of making a STT disappeared ($P > 0.1$, binomial test). The manner in which the differences disappeared, however, was not as we had predicted. If the earlier, more frequent STTs seen for tilted bars were driven solely by factors related to motion signals, we would have expected to see the tilted bar distributions shift rightward to look more like that for the nontilted bars. But, in fact, the opposite occurred: the nontilted bar distribution shifted to the left to match that of the tilted bars.

This might be explained by the fact that, when the bar was not moving, there was nothing for the animal to do for the 1-s duration of the trial, prior to receiving his reward. Under these conditions, it was perhaps not surprising that he explored the figure before him as human observers are known to do for a variety of static figures (Yarbus 1967). Moreover, the lack of movement, occurring as it did on only 20% of the trials, may have come as something of a surprise to the monkey and as such motivated enhanced exploratory behavior. Whatever the

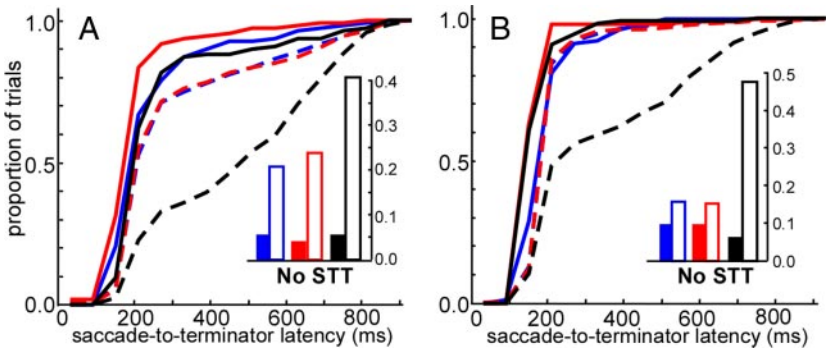

FIG. 13. Comparison of STTs to moving and stationary bars. Data are from *monkey I* and show STT cumulative distribution functions (as described in the legend to Fig. 12) for 2 different bar lengths, 9.4° (*A*) and 18.8° (*B*) for trials on which the bars either moved (dashed lines, hollow bars) or remained stationary (solid lines and bars). For all plots, blue indicates trials on which the bar was tilted +45°; red, −45°; and nontilted, black. Saccade probabilities and numbers of trials for the nontilted bar distributions (black) are given in Table 5.

case, it is known that saccade patterns are determined by a variety of visual cues. For our purpose, however, the critical distinction is that the *differences* in behavior to tilted versus nontilted bars that are so evident for moving bars are not seen for bars that are not moving.

As a second test of the role that geometry might have played, we performed a series of experiments in one monkey (*F*) in which the moving bar was always the same shape—a horizontally oriented bar—but it moved in one of six directions on any given trial, thus creating different relationships between the direction of motion and its relative orientation. The various relationships are upward and downward motion, corresponding to the no-tilt condition, up-right and down-left motion, corresponding to +45° tilt, and up-left and down-right motion, corresponding to −45° tilt (Fig. 14*A*).

Again, the data reveal the same basic pattern of STTs (Fig. 14, *B–D*). The raw eye movement traces (Fig. 14*B*) are from the same monkey (*F*) and correspond approximately in direction to those from Fig. 10*A*, and the similarity of the result is apparent. This was also true for the corresponding 2D saccade maps (compare Fig. 10, *C* and *D*, with Fig. 14, *C* and *D*). One significant difference that we did not see in our previous experiments was that the STT latency distribution for bars tilted +45° was shifted to the right of that for −45° (Fig. 14*E*, $P < 0.0001$ Wilcoxon rank-sum test). However, given that, for this experiment, the different relative tilts were confounded with different directions of bar motion, it is likely that the aforementioned directional biases for saccades combined with the bias toward leading terminators, contributed to this result. And although the latency histograms showed a difference between the +45 and −45° conditions, there was no difference with respect to the probability of never making a STT (Fig. 14*E*; $P = 0.29$, binomial test) even though each tilted condition differed dramatically from the nontilted condition ($P < 0.01$, binomial test).

In general, then, these results and those obtained with stationary bars, argue against a major contribution of static geometry and support the idea that the differences in saccade behavior engendered by bars of different relative tilts is largely produced by the discrepancy in local motion signals they present to the visual system.

DISCUSSION

We used tilted bar stimuli, which present a conflict between locally measured contour- and terminator-derived motion signals, to study the temporal evolution of 2D motion signals used to guide smooth pursuit eye movements and saccades. The conflict arises because the pursuit system obtains visual information from neurons with relatively small receptive fields that are subject to the "aperture problem," (Marr and Ullman 1981) resulting in local velocity measurements that are confounded with local contour orientation. Our results indicate that smooth pursuit is initially informed by the relatively *nonselective* pooling of local motion measurements, with the true 2D object velocity becoming apparent more gradually. This temporal evolution toward a 2D representation of motion is consistent with previous results from human direction judgments (Lorençeau et al. 1993), the human ocular following response (Masson and Castet 2002; Masson et al. 2000), smooth pursuit in monkeys (Pack and Born 2001) and humans (Lindner and Ilg 2000; Masson and Stone 2002), and the responses of MT neurons in alert monkeys (Pack and Born 2001; Pack et al. 2004). The present study has extended the observations of this phenomenon over two important stimulus parameters—contour length and eccentricity—and has begun to quantify higher level influences on bottom-up motion processing. Finally, the analysis of saccades made to moving bars has revealed a special salience of moving terminators, particularly under circumstances in which there is a discrepancy among local motion signals belonging to a single object.

How are local motion signals combined?

Our results show that both terminator- and contour-related motion signals contribute to the earliest phase of pursuit initiation. If the initial responses were driven solely by contour information, the initial angular deviation of pursuit would have been 45° regardless of the length of the bar. This was definitely not the case (Fig. 4) as short bars produced small maximum deviations (~15° deviation for bars 4.2° long) and the deviation increased monotonically with the addition of contour

TABLE 5. *Median STT latencies (s) and the probabilities of not making a STT for non-tilted bars that were either stationary (S) or moving (M)*

	Monkey J		*Monkey J*		*Monkey I*		*Monkey I*	
	STT latency		P (No STT)		STT latency		Prob (No STT)	
Bar Length	S	M	S	M	S	M	S	M
9.4	0.180	0.232	0.335	0.600	0.226	0.508	0.061	0.442
18.8	0.282	0.522	0.482	0.800	0.176	0.252	0.061	0.432
N	110	220	110	220	115	457	115	457

All comparisons between stationary and moving bars showed highly significant difference in the predicted direction ($P < 0.01$, Wilcoxon rank-sum test on latency distributions; binomial test for probabilities of no STT).

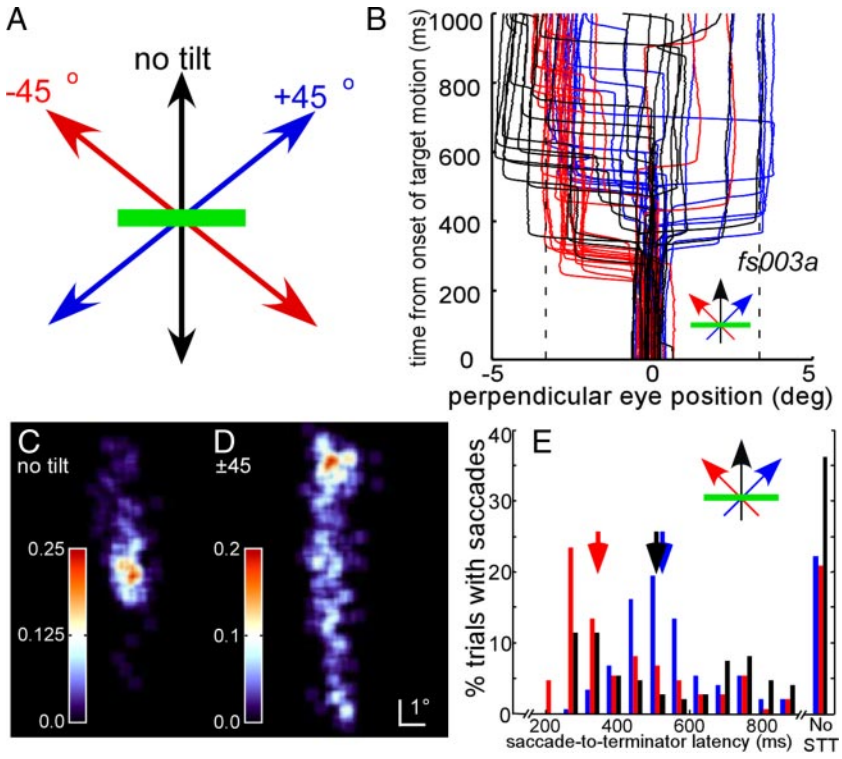

FIG. 14. STTs to horizontal bars moving in different directions. *A*: geometry of the experiment indicating the relative tilts corresponding to different directions of motion of the horizontal bar. *B*: raw eye position traces of 20 trials each from 3 different directions of bar motion: up-right (blue), up (black), and up-left (red) in which the position coordinates for each trial type have been rotated such that upwards on the *y* axis corresponds to the direction of target motion in each case. This renders the data comparable to that of Fig. 10*A*, even though the conditions were strictly identical only for the nontilted (black) condition. *C*: 2-dimensional saccade map for early saccades (between 100 and 400 ms after the bar began moving) to nontilted bars (151 saccades). *D*: saccade map for early saccades to tilted bars (232 saccades). *E*: STT latency histograms for *monkey F* for 9.4° long horizontal bars. Each condition of relative tilt consists of 150 trials. The median latencies are indicated by arrows.

signals, approaching 45° for the longest bars. Such behavior is generally consistent with a *vector average* model for combining local measurements, which has been proposed previously (Born et al. 2000; Groh et al. 1997; Lisberger and Ferrera 1997; Masson and Castet 2002; Recanzone and Wurtz 1999; Wilson and Kim 1994). This model was engendered by results from two different types of experiment. In the first, two potential pursuit targets were presented simultaneously (Lisberger and Ferrera 1997; Recanzone and Wurtz 1999); in the second, a single visual target interacted with a velocity signal elicited by microstimulation in MT (Born et al. 2000; Groh et al. 1997). In both cases, the velocity of the resulting pursuit was best modeled as the average of two velocity vectors: either those of the two visual targets (Lisberger and Ferrera 1997; Recanzone and Wurtz 1999) or that of the visual target and that of an "electrical" velocity vector introduced by microstimulation (Born et al. 2000; Groh et al. 1997).

In a variation on the two-target pursuit experiments, it was shown that attention could significantly affect the integration process. If the animal was supplied with prior knowledge concerning which target was to be pursued, it was able to suppress the motion vector from the irrelevant target thus producing a winner-take-all pursuit response (Ferrera and Lisberger 1995). However, even when target selection was made possible, the earliest pursuit response was a vector average and the attentional effects appeared only after some time (Recanzone and Wurtz 1999). In these experiments, the two potential targets were of different shapes and the animal was required to pursue the one matching the shape of a cue shown before the trial. When the two stimuli ("target" and "distracter") appeared close to each other and for only a short time (150 ms) before the animal was instructed to make the eye movement, the resulting pursuit was again a vector average of the two velocity vectors. If, however, target and distracter appeared further apart and for a longer time (450 ms) before the cue to make the eye movement, pursuit occurred as if the appropriate target were the only stimulus present.

This ability of attention to suppress behaviorally irrelevant motion signals suggests one possible mechanism for the solution of the aperture problem. Interpreted in this way, the pursuit behavior evolves from an initial vector-average of all local motion signals to a winner-take-all solution in which the terminator signals win through attentional enhancement of the terminator signals, suppression of the contour signals, or a combination of both. The temporal dynamics of this process may therefore reflect the timing of attentional shifts (Krose and Julesz 1989; Saarinen and Julesz 1991; Verstraten et al. 2000).

Alternatively, the timing of the behavior might be determined in a more "bottom-up" fashion by the properties of visual neurons early in the pursuit pathway. One such possibility was suggested by recent recordings from striate cortex of alert monkeys, which revealed a temporal delay in the emergence of end-stopping in direction-selective neurons (Pack et al. 2003). From this perspective, the temporal evolution of 2D motion signals for pursuit and those that have been observed in MT neurons (Pack and Born 2001; Pack et al. 2004) would not reflect a change in the underlying computation—a vector average would always suffice—but rather a change in the "weighting" applied to the outputs of V1 direction-selective neurons as end-stopping eventually suppresses contour-related motion signals and emphasizes those from terminators. Such a mechanism might also explain the perceptual dominance of a contour-vector average for stimuli of *low contrast* (Weiss et al. 2002), since end-stopping is weak or absent for such stimuli (Polat et al. 1998; Sceniak et al. 1999). This strikes us as a parsimonious explanation of much of the existing data from perceptual, behavioral, and single-unit studies. Moreover, it is physiologically very plausible given the fact that neurons

comprising the predominant source of cortical input to the pursuit pathway, those in layer 4B of V1 (Maunsell and Van Essen 1983; Shipp and Zeki 1989), are also strongly end-stopped (Sceniak et al. 2001).

Properties of the integration "window"

The experiments in which we systematically varied the length of the bar (Fig. 4) make it clear that the initial integration can take place over a large spatial range—up to 34°—and very quickly, as the effect of bar length was manifest as soon as the eyes began to move. This finding is consistent with previous studies of the effects of field size on smooth eye movements in which considerable integration over space has also been observed (Heinen and Watamaniuk 1998; Pola and Wyatt 1985).

Proposing such a potentially large integration window for pursuit might appear heterodox since pursuit is generally taken to be a behavior specialized for tracking *small* targets (Carpenter 1988; Ilg 1997). Looked at another way, one might wonder if what we have measured in our experiments is really smooth pursuit or some other form of visually evoked smooth eye movement, such as ocular following. Clearly our subjects were required to track a single object, and the general characteristics of their eye movements, with the notable exception of the contour-induced *deviation*, changed little as the target was varied from something quite small (a bar $<0.5°$ wide by 4° long) to something very large (a parallelogram more than 12° wide by more than 30° long). It thus appears to us that the boundary between pursuit and other types of smooth eye movements is a fuzzy one.

This may not be all that surprising given that the anatomical substrates of the various smooth eye-movement pathways are largely overlapping (Ilg 1997) with many neurons at cortical and subcortical stages of the pathways responding to the motion of both small spots and large textured fields, as well as during pursuit and optokinetic eye movements (Heinen and Keller 1996; Hoffmann and Distler 1989; Komatsu and Wurtz 1988; Mustari and Fuchs 1989; Suzuki and Keller 1988). Moreover, previous investigators have noted the similarities in basic properties among so-called early OKN, ocular following, and the initiation of smooth pursuit (Carpenter 1988; Ilg 1997; Miles et al. 1991). The crucial difference would seem to be that pursuit can involve the *voluntary* selection of certain motion signals over others (Khurana and Kowler 1987; Miles et al. 1991). This is consistent with our findings on the variability of the size and shape of the integration window for pursuit initiation as well as the ability of predictability to mitigate the contour effect. These same experiments also make clear, however, that the ability of the pursuit system to select some motion signals over others is not absolute, at least not for pursuit initiation.

Retinotopy of sensory maps informing pursuit

The eccentricity of the various local motion signals had only a modest effect on the contour-induced deviation of pursuit, and practically no effect on the early component (Figs. 6–8). For the late component of pursuit, we interpret the decline in contour-induced deviation with eccentricity to indicate the effect of integrating the responses of neurons with progressively larger receptive fields, as schematized in Fig. 5*A*. With increasing receptive field size of the inputs to the vector-averaging stage, the coarser sampling effectively shrinks the bar and decreases the relative contribution of the contour-based motion signals.

The differential sensitivity to eccentricity of the different temporal phases of pursuit initiation is reminiscent of a similar difference found for open-loop eye acceleration to spot targets (Lisberger and Westbrook 1985). In these experiments, the investigators found that the "early component" of pursuit initiation (the 1st 40 ms) was largely unaffected by the initial target position with respect to the fovea, whereas the "late component" (the 2nd 40 ms of pursuit) was strongly affected by this parameter. The contour-induced deviation measured here was similar with respect to contour eccentricity and further supports the idea that the early phase of pursuit initiation is driven by inputs that de-emphasize the central visual fields (Morris and Lisberger 1987) or, alternatively, have uniformly large receptive fields across the representation of visual space—such as those found in the accessory optic system (Simpson 1984). The later phase of pursuit initiation might then reflect contributions from one or more pathways involving MT, the retinotopic map of which places a greater emphasis on foveal vision (Gattass and Gross 1981; Van Essen et al. 1981).

Top-down versus bottom-up

For monkeys, the effects of predictability were rather small, but clearly present, particularly when stimulus direction was held constant across blocks of trials (Fig. 9). This result is generally consistent with previous experiments in which evidence for "predictive" pursuit has been found in monkeys (Deno et al. 1995; Domann et al. 1989; Eckmiller and Mackeben 1978; Heinen and Liu 1997). Our experiments, however, differed from previous studies in several important ways. First, most of the previous work has examined the *steady-state* pursuit of more- versus less-predictable target motions. Second, the only study of which we're aware that examined predictive effects on pursuit initiation in *monkeys* found an effect on the *latency* of pursuit (Domann et al. 1989). In this case, the predictive signal was the monkey's own intent to move—target motion was controlled by the subject's arm motion—and the local motion signals generated by the target were not in conflict. In our experiments, the predictive signal was pitted against visual signals that were themselves in conflict to ask to what extent it could mitigate the effect of ambiguous local signals. Thus for our experiments, predictive signals had to override a visual signal rather than simply anticipate its occurrence in time.

Salience of terminators

When monkeys are presented with long bars as pursuit targets, they naturally tend to make saccades to the bar's endpoints. This behavior struck us as interesting, so we measured it in animals that were experts at pursuing spots but that were naïve with respect to bar pursuit. The results (Figs. 10–14) supported our anecdotal observations made during the training of the other monkeys and revealed potentially important features of the visual tracking system under natural con-

ditions. First, there was a tendency for the animal to saccade to the bars' endpoints regardless of the relative orientation, suggesting a particular salience of discontinuities. In our initial experiments, there were actually two discontinuities between the bar and the background—one in luminance and the other in velocity—and either one or both could have increased the salience of the endpoints. Clearly, in the absence of motion, the luminance discontinuities sufficed to attract saccades to terminators (Fig. 13). However, neither the luminance nor the motion discontinuity can explain the fact that the monkey was more likely to saccade to the endpoints and to do so at shorter latency, when the bar's orientation was oblique *with respect to its direction of motion*. This result is most simply explained by the *variation* in the direction of local motion signals between contours and terminators that belong to the same object. The fact that the *differences* between tilted and nontilted bars disappeared when the bars were stationary (Fig. 13) and were independent of a particular geometry (Fig. 14) further underscore the importance of the motion cues.

Our finding that many of the saccades-to-terminators elicited by tilted bars occurred at very short latencies suggests some relatively fast calculation of variance in local motion signals. We have already remarked on the suitability of end-stopped, direction-selective neurons in V1 for representing the motion of terminators (Hubel and Wiesel 1965; Pack et al. 2003). It is quite conceivable, however, that the direction of contour motion is also explicitly represented, perhaps by the large Meynert cells found between layers 5 and 6 in V1, which are direction-selective (Movshon and Newsome 1996) and known to project to MT (Maunsell and Van Essen 1983; Shipp and Zeki 1989) but are probably *not* end-stopped (Movshon and Newsome 1996; Sceniak et al. 2001). If this was the case, a quick "consistency check" might easily be performed by comparing the direction preferences of the two populations activated by a given stimulus. Such a comparison might be realized, possibly in V1 or MT, if the horizontal intrinsic connections between groups of direction-selective neurons were to follow the same rule—essentially one of "like to like"—as that for orientation columns in V1 (Bosking et al. 1997; Gilbert and Wiesel 1989; Malach et al. 1993; Weliky et al. 1995). For example, a vertical bar moving to the right would activate directionally corresponding (i.e., rightward preferring)—and thus likely, interconnected—populations of neurons in both layers 4B and 6, whereas a bar tilted +45° would activate directionally disparate populations (rightwards in layer 4B, up-right in layer 6). The result of the comparison could then influence saccade behavior, either directly, through the projection of the V1 Meynert cells (the same ones projecting to MT) to the superior colliculus (Fries et al. 1985) or that from MT to the superior colliculus (Maunsell and Van Essen 1983; Ungerleider et al. 1984) or indirectly via MT's connections with posterior parietal areas involved in saccade programming, such as LIP (Andersen et al. 1990; Lewis and Van Essen 2000).

ACKNOWLEDGMENTS

We gratefully acknowledge the technical assistance of P. Hendrickson. For helpful comments on the manuscript, we thank J. Assad and M. Livingstone.

GRANTS

This work was supported by National Institutes of Health Grants EY-1379, EY-12196, and BCS-0235398 and by grants from the Whitehall Foundation and the Centre National de la Recherche Scientifique.

REFERENCES

Andersen RA, Asanuma C, Essick G, and Siegel RM. Corticocortical connections of anatomically and physiologically defined subdivisions within the inferior parietal lobule. *J Comp Neurol* 296: 65–113, 1990.

Born RT, Groh JM, Zhao R, and Lukasewycz SJ. Segregation of object and background motion in visual area MT: effects of microstimulation on eye movements. *Neuron* 26: 725–734, 2000.

Born RT and Pack CC. Integration of motion signals for smooth pursuit eye movements. *Ann NY Acad Sci* 956: 453–455, 2002.

Born RT, Pack CC, and Zhao R. Integration of motion cues for the initiation of smooth pursuit eye movements. *Prog Brain Res* 140: 225–237, 2002.

Bosking WH, Zhang Y, Schofield B, and Fitzpatrick D. Orientation selectivity and the arrangement of horizontal connections in tree shrew striate cortex. *J Neurosci* 17: 2112–2127, 1997.

Carl JR and Gellman RS. Human smooth pursuit: stimulus-dependent responses. *J Neurophysiol* 57: 1446–1463, 1987.

Carpenter RHS. *Movements of the Eyes.* London: Pion, 1988.

CIE. *Commission Internationale de l'Éclairage Proceedings, 1931.* Cambridge, UK: Cambridge Univ. Press, 1932.

Daniel PM and Whitteridge D. The representation of the visual field on the cerebral cortex in monkeys. *J Physiol* 159: 203–221, 1961.

Deno DC, Crandall WF, Sherman K, and Keller EL. Characterization of prediction in the primate visual smooth pursuit system. *Biosystems* 34: 107–128, 1995.

Domann R, Bock O, and Eckmiller R. Interaction of visual and non-visual signals in the initiation of smooth pursuit eye movements in primates. *Behav Brain Res* 32: 95–99, 1989.

Draper NR and Smith H. *Applied Regression Analysis.* New York: Wiley, 1966.

Eckmiller R and Mackeben M. Pursuit eye movements and their neural control in the monkey. *Pfluegers Eur JPhysiol* 377: 15–23, 1978.

Efron B and Tibshirani RJ. *An Introduction to the Bootstrap.* New York: Chapman and Hall, 1993.

Ferrera VP and Lisberger SG. Attention and target selection for smooth pursuit eye movements. *J Neurosci* 15: 7472–7484, 1995.

Fries W, Keizer K, and Kuypers HG. Large layer VI cells in macaque striate cortex (Meynert cells) project to both superior colliculus and prestriate visual area V5. *Exp Brain Res* 58: 613–616, 1985.

Fuchs AF. Periodic eye tracking in the monkey. *J Physiol* 193: 161–171, 1967.

Gattass R and Gross CG. Visual topography of striate projection zone (MT) in posterior superior temporal sulcus of the macaque. *J Neurophysiol* 46: 621–638, 1981.

Gilbert CD and Wiesel TN. Columnar specificity of intrinsic horizontal and corticocortical connections in cat visual cortex. *J Neurosci* 9: 2432–2442, 1989.

Groh JM, Born RT, and Newsome WT. How is a sensory map read out? Effects of microstimulation in visual area MT on saccades and smooth pursuit eye movements. *J Neurosci* 17: 4312–4330, 1997.

Heinen SJ and Keller EL. The function of the cerebellar uvula in monkey during optokinetic and pursuit eye movements: single-unit responses and lesion effects. *Exp Brain Res* 110: 1–14, 1996.

Heinen SJ and Liu M. Single-neuron activity in the dorsomedial frontal cortex during smooth-pursuit eye movements to predictable target motion. *Vis Neurosci* 14: 853–865, 1997.

Heinen SJ and Watamaniuk SN. Spatial integration in human smooth pursuit. *Vision Res* 38: 3785–3794, 1998.

Hoffmann KP and Distler C. Quantitative analysis of visual receptive fields of neurons in nucleus of the optic tract and dorsal terminal nucleus of the accessory optic tract in macaque monkey. *J Neurophysiol* 62: 416–428, 1989.

Hubel DH and Wiesel TN. Receptive fields and functional architecture in two non-striate visual areas (18 and 19) of the cat. *J Neurophysiol* 28: 229–289, 1965.

Ilg UJ. Slow eye movements. *Prog Neurobiol* 53: 293–329, 1997.

Judge SJ, Richmond BJ, and Chu FC. Implantation of magnetic search coils for measurement of eye position: an improved method. *Vision Res* 20: 535–538, 1980.

Khurana B and Kowler E. Shared attentional control of smooth eye movement and perception. *Vision Res* 27: 1603–1618, 1987.

Komatsu H and Wurtz RH. Relation of cortical areas MT and MST to pursuit eye movements. I. Localization and visual properties of neurons. *J Neurophysiol* 60: 580–603, 1988.

Komatsu H and Wurtz RH. Modulation of pursuit eye movements by stimulation of cortical areas MT and MST. *J Neurophysiol* 62: 31–47, 1989.
Krauzlis RJ and Miles FA. Release of fixation for pursuit and saccades in humans: evidence for shared inputs acting on different neural substrates. *J Neurophysiol* 76: 2822–2833, 1996.
Krose BJ and Julesz B. The control and speed of shifts of attention. *Vision Res* 29: 1607–1619, 1989.
Lewis JW and Van Essen DC. Corticocortical connections of visual, sensorimotor, and multimodal processing areas in the parietal lobe of the macaque monkey. *J Comp Neurol* 428: 112–137, 2000.
Lindner A and Ilg UJ. Initiation of smooth-pursuit eye movements to first-order and second-order motion stimuli. *Exp Brain Res* 133: 450–456, 2000.
Lisberger SG and Ferrera VP. Vector averaging for smooth pursuit eye movements initiated by two moving targets in monkeys. *J Neurosci* 17: 7490–7502, 1997.
Lisberger SG, Morris EJ, and Tychsen L. Visual motion processing and sensory-motor integration for smooth pursuit eye movements. *Annu Rev Neurosci* 10: 97–129, 1987.
Lisberger SG and Westbrook LE. Properties of visual inputs that initiate horizontal smooth pursuit eye movements in monkeys. *J Neurosci* 5: 1662–1673, 1985.
Lorençeau J, Shiffrar M, Wells N, and Castet E. Different motion sensitive units are involved in recovering the direction of moving lines. *Vision Res* 33: 1207–1217, 1993.
Madelain L and Krauzlis RJ. Pursuit of the ineffable: perceptual and motor reversals during the tracking of apparent motion. *J Vis* 3: 642–653, 2003.
Malach R, Amir Y, Harel M, and Grinvald A. Relationship between intrinsic connections and functional architecture revealed by optical imaging and in vivo targeted biocytin injections in primate striate cortex. *Proc Natl Acad Sci USA* 90: 10469–10473, 1993.
Marr D and Ullman S. Directional selectivity and its use in early visual processing. *Proc R Soc Lond B Biol Sci* 211: 151–180, 1981.
Masson GS and Castet E. Parallel motion processing for the initiation of short-latency ocular following in humans. *J Neurosci* 22: 5149–5163, 2002.
Masson GS, Rybarczyk Y, Castet E, and Mestre DR. Temporal dynamics of motion integration for the initiation of tracking eye movements at ultra-short latencies. *Vis Neurosci* 17: 753–767, 2000.
Masson GS and Stone LS. From following edges to pursuing objects. *J Neurophysiol* 88: 2869–2873, 2002.
Maunsell JH and Van Essen DC. The connections of the middle temporal visual area (MT) and their relationship to a cortical hierarchy in the macaque monkey. *J Neurosci* 3: 2563–2586, 1983.
Miles FA, Schwarz U, and Busettini C. The parsing of optic flow by the primate oculomotor system. In: *Representations of Vision: Trends and Tacit Assumptions in Vision Research,* edited by Gorea A. Cambridge, UK: Cambridge Univ. Press 1991, p. 185–199.
Morris EJ and Lisberger SG. Different responses to small visual errors during initiation and maintenance of smooth-pursuit eye movements in monkeys. *J Neurophysiol* 58: 1351–1369, 1987.
Movshon JA and Newsome WT. Visual response properties of striate cortical neurons projecting to area MT in macaque monkeys. *J Neurosci* 16: 7733–7741, 1996.
Mustari MJ and Fuchs AF. Response properties of single units in the lateral terminal nucleus of the accessory optic system in the behaving primate. *J Neurophysiol* 61: 1207–1220, 1989.
Newsome WT, Wurtz RH, Dursteler MR, and Mikami A. Deficits in visual motion processing following ibotenic acid lesions of the middle temporal visual area of the macaque monkey. *J Neurosci* 5: 825–840, 1985.
Pack CC, Berezovskii VK, and Born RT. Dynamic properties of neurons in cortical area MT in alert and anaesthetized macaque monkeys. *Nature* 414: 905–908, 2001.
Pack CC and Born RT. Temporal dynamics of a neural solution to the aperture problem in visual area MT of macaque brain. *Nature* 409: 1040–1042, 2001.
Pack CC, Gartland AJ, and Born RT. Integration of contour and terminator signals in visual area MT of alert macaque. *J Neurosci* 24: 3268–3280, 2004.
Pack CC, Livingstone MS, Duffy KR, and Born RT. End-stopping and the aperture problem: two-dimensional motion signals in macaque V1. *Neuron* 39: 671–680, 2003.
Pola J and Wyatt HJ. Active and passive smooth eye movements: effects of stimulus size and location. *Vision Res* 25: 1063–1076, 1985.
Polat U, Mizobe K, Pettet MW, Kasamatsu T, and Norcia AM. Collinear stimuli regulate visual responses depending on cell's contrast threshold. *Nature* 391: 580–584, 1998.
Rashbass C. The relationship between saccadic and smooth tracking eye movements. *J Neurophysiol* 159: 326–338, 1961.
Recanzone GH and Wurtz RH. Shift in smooth pursuit initiation and MT and MST neuronal activity under different stimulus conditions. *J Neurophysiol* 82: 1710–1727, 1999.
Robinson DA. A method of measuring eye movement using a scleral search coil in a magnetic field. *IEEE Trans Biomed Eng* 10: 137–145, 1963.
Saarinen J and Julesz B. The speed of attentional shifts in the visual field. *Proc Natl Acad Sci USA* 88: 1812–1814, 1991.
Sceniak MP, Hawken MJ, and Shapley R. Visual spatial characterization of macaque V1 neurons. *J Neurophysiol* 85: 1873–1887, 2001.
Sceniak MP, Ringach DL, Hawken MJ, and Shapley R. Contrast's effect on spatial summation by macaque V1 neurons. *Nat Neurosci* 2: 733–739, 1999.
Shipp S and Zeki S. The organization of connections between areas V5 and V1 in macaque monkey visual cortex. *Eur J Neurosci* 1: 309–332, 1989.
Simpson JI. The accessory optic system. *Annu Rev Neurosci* 7: 13–41, 1984.
Suzuki DA and Keller EL. The role of the posterior vermis of monkey cerebellum in smooth-pursuit eye movement control. II. Target velocity-related Purkinje cell activity. *J Neurophysiol* 59: 19–40, 1988.
Trujillo-Ortiz A, Hernandez-Walls R, and Trujillo-Perez, RA. RMAOV1: one-way repeated measures ANOVA. A MATLAB file. Web page, [accessed 28 February 2005]. Available at http://www.mathworks.com/matlabcentral/fileexchange/loadFile.do?objectId=5576, 2004a.
Trujillo-Ortiz A, Hernandez-Walls R, and Trujillo-Perez, RA. RMAOV2: two-way repeated measures ANOVA. A MATLAB file. Web page, [accessed 28 February 2005]. Available at http://www.mathworks.com/matlabcentral/fileexchange/loadFile.do?objectId=5578, 2004b.
Ungerleider LG, Desimone R, Galkin TW, and Mishkin M. Subcortical projections of area MT in the macaque. *J Comp Neurol* 223: 368–386, 1984.
Van Essen DC, Maunsell JH, and Bixby JL. The middle temporal visual area in the macaque: myeloarchitecture, connections, functional properties and topographic organization. *J Comp Neurol* 199: 293–326, 1981.
Verstraten FA, Cavanagh P, and Labianca AT. Limits of attentive tracking reveal temporal properties of attention. *Vision Res* 40: 3651–3664, 2000.
von Grunau MW, Bertone, A, and Pakneshan, P. Attentional selection of motion states. *Spat Vis* 11: 329–347, 1998.
Weiss Y, Simoncelli EP, and Adelson EH. Motion illusions as optimal percepts. *Nat Neurosci* 5: 598–604, 2002.
Weliky M, Kandler K, Fitzpatrick D, and Katz LC. Patterns of excitation and inhibition evoked by horizontal connections in visual cortex share a common relationship to orientation columns. *Neuron* 15: 541–552, 1995.
Wilson HR and Kim J. Perceived motion in the vector sum direction. *Vision Res* 34: 1835–1842, 1994.
Yarbus AL. *Eye Movements and Vision.* New York: Plenum. 1967.
Zar JH. *Biostatistical Analysis.* NJ: Prentice-Hall. 1996.